

Contents lists available at ScienceDirect

Palaeogeography, Palaeoclimatology, Palaeoecology

journal homepage: www.elsevier.com/locate/palaeo





Late Permian soil-forming paleoenvironments on Gondwana: A review

Erik L. Gulbranson^{a,*}, Nathan D. Sheldon^b, Isabel P. Montañez^c, Neil J. Tabor^d, Julia A. McIntosh^d

- ^a Department of Geology, Gustavus Adolphus College, 56082, USA
- ^b Department of Earth and Environmental Sciences, University of Michigan, 48109, USA
- c Department of Earth and Planetary Sciences, University of California Davis, 95616, USA
- ^d Roy M. Huffington Department of Earth Sciences, Southern Methodist University, 75205, USA

ARTICLE INFO

Editor: Prof. Thomas Algeo

Keywords: Paleosols Paleoclimate Mass extinction Geochemistry

ABSTRACT

Paleosols represent fossil records of paleolandscape processes, paleobiotic interactions with the land surface, and paleoclimate. Paleosol-based reconstructions have figured prominently in the study of significant changes in global climate and terrestrial life, with one of the more highly studied examples being the end-Permian extinction (EPE). The EPE was once thought to consist of synchronous extinctions in the marine realm and the terrestrial realm, with the latter displaying a lower magnitude extinction of vertebrate, insect, and plant life. However, emerging stratigraphic records, anchored by high-precision U—Pb ages, and compilations of fossil taxa indicate that the terrestrial realm on Gondwana experienced an asynchronous extinction record with the marine realm; and, at the global-scale, possibly the lack of a true mass extinction for plant and vertebrate communities. Moreover, paleosol-based interpretations of the EPE on Gondwana typically focus on one depositional basin and extrapolate those finding to assess the potential for global paleoenvironmental/paleoclimatic change. This review compiles observations of paleosols, sedimentology, stratigraphy, and geochemical data across Gondwana during the Late Permian in order to critically assess these interpretations of global change in the lead up to the FPF

1. Introduction

Paleosols, fossils soils that preserve a part of the original soil environment, are long recognized as vital components of paleoclimate reconstructions (Simonson, 1941; Bryan and Albritton, 1943; Retallack, 1988; Mack et al., 1993; Kraus, 1999; Sheldon and Tabor, 2009). Basin-specific or regional paleoclimate reconstructions often are derived from the analysis of paleosols (Table 1; Alonso-Zarza et al., 1992; Kraus, 2002; Tabor and Montañez, 2004; Hartley et al., 2013; Weissmann et al., 2010, 2013; Gulbranson et al., 2015a; Michel et al., 2015), including applications of geochemical climate proxies (Mora et al., 1996; Driese et al., 2000; Sheldon et al., 2002; Ekart et al., 1999; Ghosh et al., 2006; Montañez et al., 2007; Passey et al., 2010; Meyers et al., 2012; Montañez, 2013; Quade et al., 2013; Dzombak et al., 2020). At a smaller scale, it is vital to report the characteristics of paleosols in a vertical succession of strata against the broader context of the lateral variation of soil, sedimentary, and paleoecologic systems in order to differentiate

between regional controls on soil development from autogenic relationships among the state factors for soil formation (Bown and Kraus, 1987; McDonald and Busacca, 1990; Ashley and Driese, 2000; Driese et al., 2005; Gastaldo et al., 2014). At this smaller scale, the (paleo-) catena concept (Valentine and Dalrymple, 1975), is an ideal type of geospatial analysis of paleosols (preservation-permitting) that permits assessing non-climatic controls on soil formation based on landscape position, hydrology, and ecology; which represents more of an Earth Systems style analysis of paleosols (Bown and Kraus, 1987; Besly and Fielding, 1989; Kraus and Aslan, 1993; Kraus, 1999; Dzombak et al., 2021). The focus of the paleo-catena concept is the recognition of significant variance in physical and chemical soil properties occur and are interconnected on a landscape via soil drainage conditions; habitat variance; and the balance of landscape erosion and deposition. By applying Walther's Law to this concept it is expected that vertical changes in soil physical and chemical properties will occur based on shifting landscape positions through time in the sedimentary system in

E-mail addresses: erikgulbranson@gustavus.edu (E.L. Gulbranson), nsheldon@umich.edu (N.D. Sheldon), ipmontanez@ucdavis.edu (I.P. Montañez), ntabor@mail.smu.edu (N.J. Tabor), mcintoshj@mail.smu.edu (J.A. McIntosh).

^{*} Corresponding author.

addition to temporal variations in biota and climate. Thus, elucidating the non-climatic state factors of the soil-forming system in a vertical succession of paleosols is vitally important if paleosols are to faithfully and unambiguously demonstrate a temporal record of paleoclimate change.

One of the most high-profile paleosol-based paleoclimate and paleoenvironmental interpretations centers on the discussion of the end-Permian extinction (EPE) and Early-Middle Triassic recovery of terrestrial ecosystems (Table 1). However, these paleosol-focused studies have focused on individual basins, to either decipher the intricacies of paleosol formation and depositional setting (Table 1); or to draw broad, and global-scale, conclusions about terrestrial environmental and ecologic change in the lead up to the EPE, during the EPE, and the Early Triassic aftermath (Krull and Retallack, 2000; Ward et al., 2000, 2005; Huey and Ward, 2005; Smith and Botha, 2005; Retallack et al., 2006, 2011; Retallack, 2021). Since the time of publication of many of these studies, the geochronology and biostratigraphy of Upper Permian and Lower Triassic strata on Gondwana has improved remarkably, with well constrained Permian-Triassic successions in the Karoo Basin (Fig. 1B, Rubidge et al., 2013; Gastaldo et al., 2018, 2020b, 2021); the Sydney Basin (Fig. 1D, Metcalfe et al., 2015; Fielding et al., 2019); the Paganzo Basin (Fig. 1A, Gulbranson et al., 2015b); and precise biostratigraphic correlations with the eastern Australia palynoassemblages (Barbolini et al., 2016). However, much work has yet to be done to further refine: the timing of vertebrate assemblage zones and palynostratigraphy relative to the EPE in the Karoo Basin (Gastaldo et al., 2019); Permian-Triassic successions in the Paraná Basin (Fig. 1C) and the Transantarctic basins (Fig. 1E). Although Late Permian strata are reasonably welldefined through biostratigraphy and detrital zircon maximum depositional ages in both depositional settings (Collinson et al., 2006; Elliot et al., 2017; Francischini et al., 2018a; Ernesto et al., 2020). Thus, given that intensive study of paleosols occur in parts of the Karoo Basin; Sydney Basin; Transantarctic Basin; Paranà Basin and Paganzo Basin (Figs. 1 & 2), and the increasing fidelity of Earth time recorded around the Permian-Triassic transition, a review of paleosols and the paleo soil-forming environments across Gondwana during the Late Permian is possible and crucial in assessing some key interpretations of paleoclimatic and paleoecologic change during the EPE.

Several prominent paleosol-centric hypotheses of Late Permian paleoenvironmental and paleoclimate change have emerged. Aridification across the EPE has been inferred across Gondwana and reflective of perhaps a global-scale symptom of the effects of the EPE on terrestrial ecosystems based on time-equivalent comparison with the paleotropical latitudes (Ward et al., 2000, 2005; Retallack et al., 2003; Smith and Botha, 2005). In a similar vein, the assumed dearth of vegetation on land, and associated 'coal gap' (Retallack et al., 1996), has been aligned to interpretations of changes in fluvial style from high-sinuosity systems to low-sinuosity systems (Smith, 1995; Ward et al., 2000, 2005) and a "soil erosion crisis" coincident across Gondwana (Retallack et al., 2006). Paleoatmospheric oxygen content is inferred to have dropped dramatically and affecting the habitat ranges of land vertebrates (Huey and Ward, 2005), perhaps to match with the well-established shoaling oxvgen minimum zones in marine successions during the EPE (Hotinski et al., 2001; Twitchett et al., 2004; Grasby and Beauchamp, 2009; Brennecka et al., 2011; Shen et al., 2011). However, recent biogeochemical modeling demonstrates a lack of significant decrease in atmospheric pO2 during the EPE (Lenton et al., 2018). Terrestrial vegetation has been argued to have undergone a similar (Rees, 2002; Cascales-Miñana and Cleal, 2014; Cascales-Miñana et al., 2016), but lower magnitude, extinction as documented in the marine realm (Erwin, 1994; Jin et al., 2000; Bercovici et al., 2015; Yu et al., 2015; Chu et al., 2019; Retallack, 2021). There is a parallel line of evidence that supports an asynchronous extinction of terrestrial vegetation and fauna relative to the marine realm (Gastaldo et al., 2009, 2015, 2020b; Rubidge et al., 2013; Fielding et al., 2019) or perhaps a marginal decrease in diversity during the Lopingian (Sues and Fraser, 2010; Nowak et al., 2019).

Table 1
Summary of paleosols discussed in this review.

Depositional Basin	Paleosol types	Stratigraphic unit and age	Paleoclimate interpretation	Literature cited
Paganzo Basin Paraná Basin	Protosols Protosols	Talampaya Fm., Changhsingian Buena Vista Fm., Wuchiapingian–Changhsingian	Arid to semi-arid Inconclusive from paleosol morphology, sedimentary facies suggest semi-arid/ sub-humid paleoclimate	Gulbranson et al., 2015b Ernesto et al., 2020; Piñeiro et al., 2012
Karoo Basin, west of 24°E	Protosols, Vertisols, Gypsisols ¹	Teekloof Fm., Wuchiapingian	Arid, paleo catena relationship	Smith, 1990, 1995; Retallack, 2005
Karoo basin, east of 24°E	Protosols, calcic Protosols, calcic Vertisols	Balfour Fm., Elandsberg and Palingkloof members, Changhsingian	Variable paleoclimate through space and time; mixture of open-system and closed-system soil-forming conditions; variable soil hydrology across the basin	Retallack et al., 2003; Ward et al., 2005; Smith and Botha, 2005; Coney et al., 2007; Tabor et al., 2007; Gastaldo and Rolerson, 2008; Gastaldo et al., 2009; Prevec et al., 2010; Smith and Botha-Brink, 2014; Gastaldo et al., 2014, 2020a, 2020c; Li et al., 2017; Retallack, 2021
Lebombo Basin	Protosols, Histosols	Emakwezini Formation, Wuchiapingian–Changhsingian	Inconclusive from paleosol morphology, paleosol morphology and sedimentary systems suggest abundance of surface water and groundwaters	Bordy and Prevec, 2008
Transantarctic Basin (CTAM)	Protosols, Histosols	Buckley Formation (Upper Member); Fremouw Formation (Lower Member), Wuchiapingian–Changhsingian	Inconclusive from paleosol morphology, paleosol morphology and sedimentary systems suggest abundance of surface water and groundwaters	Retallack and Krull, 1999; Krull and Retallack, 2000; Sheldon, 2006; Gulbranson et al., 2012
Transantarctic Basin (SVL)	Protosols, Histosols	Weller Coal Measures, Wuchiapingian–Changhsingian	Inconclusive from paleosol morphology, paleosol morphology and sedimentary systems suggest abundance of surface water and groundwaters	Retallack and Krull, 1999; Sheldon et al., 2014; Gulbranson et al., 2020
Sydney Basin	Protosols, Histosols	Newcastle Coal Measures, Changhsingian; Illawara Coal Measures, Wuchiapingian–Changhsingian	Gelic temperature regime, however, this has not been supported by additional studies. Sedimentary facies suggest abundant surface water	Retallack, 1999a, 1999b; Retallack et al., 2011; Fielding et al., 2019; Retallack, 2021

Note: ¹The location of the paleo-catena displaying these three paleosol types has not been re-located in subsequent study and the occurrence of Gypsisols in the Teekloof Fm., Karoo Basin is uncertain.

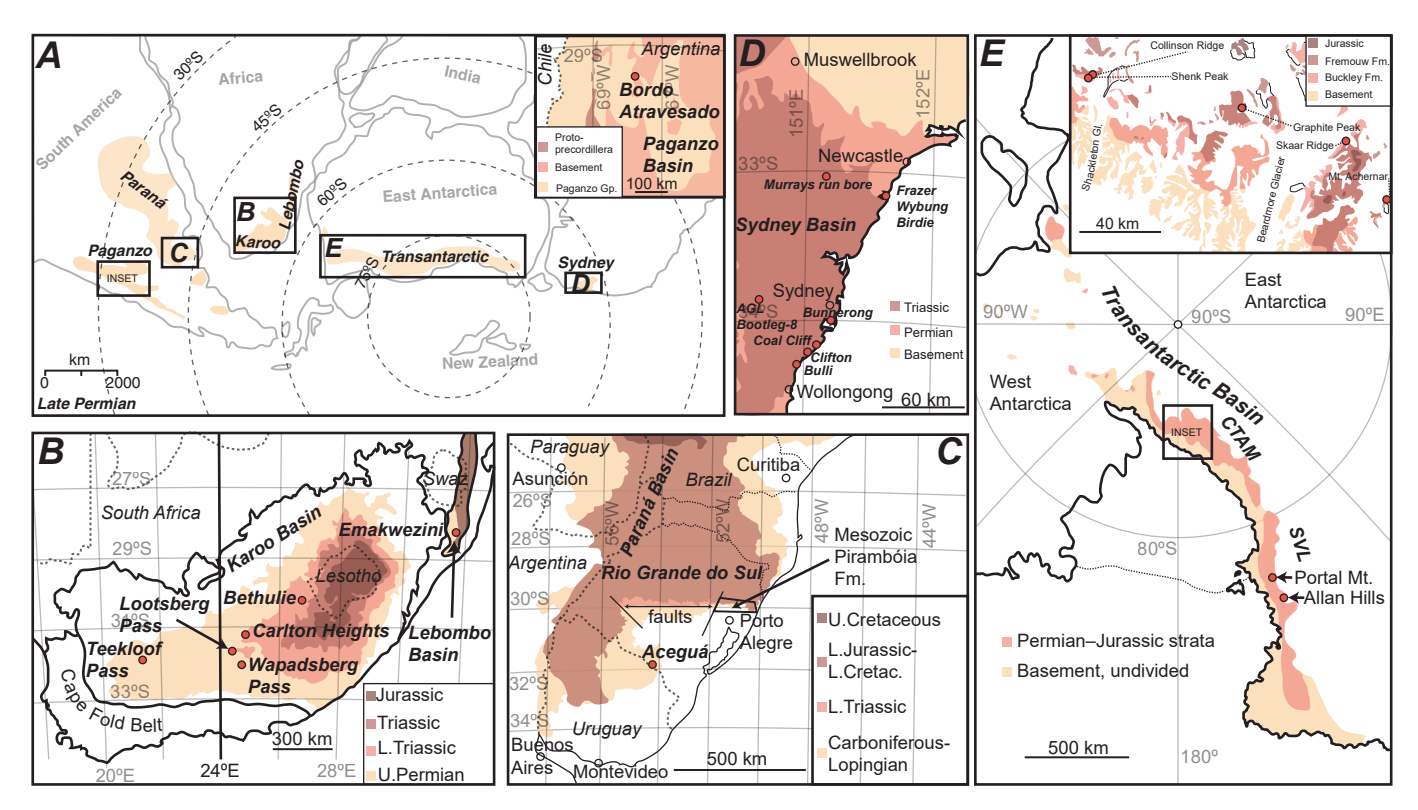


Fig. 1. Paleogeographic reconstruction and current geography of the study region, locations mentioned in the text are indicated for each geographic map. A) Paleogeographic reconstruction of Gondwana during the Lopingian, in which depositional basins are highlighted. B) Geography of the Karoo and Lebombo basins with Permian–Jurassic strata highlighted (after Coney et al., 2007; Bordy and Prevec, 2008). The 24°E meridian is basin-wide distribution between the western and eastern Karoo Basin. C) Paraná Basin geography with Carboniferous–Cretaceous stratigraphy highlighted (after Francischini et al., 2018a). Lopingian strata in Rio Grande do Sul State and Uruguay are discussed in the text. The distinction between the location of the Lopingian Pirambóia Fm. (in contact with Induan strata), and the Mesozoic Pirambóia Fm. is indicated. D) Geography of the Sydney Basin with basin-bounding basement rock and Permian–Triassic strata highlighted (after Metcalfe et al., 2015). E) Geography of the Transantarctic basins (after Collinson et al., 2006), with basin-bounding basement rocks and Permian–Jurassic strata highlighted. CTAM = central Transantarctic Mountains, SVL = southern Victoria Land. Inset image highlights key locations in the CTAM area that may contain a continuous record of the end-Permian extinction.

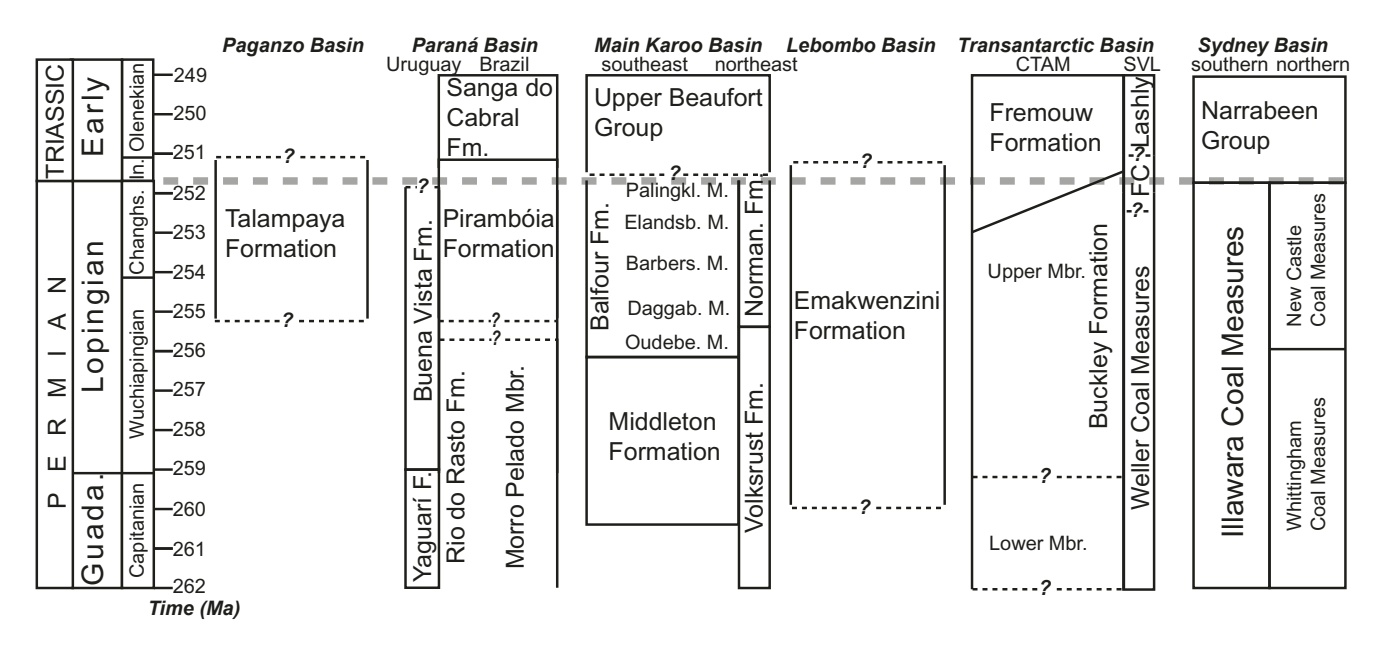


Fig. 2. Stratigraphic chart for the study region. The Permian-Triassic boundary is indicated by the horizontal dashed line. Age ranges for strata are based on discussion in the text, and where the range is uncertain are dashed with a question mark. For the Transantarctic Basin, FC=Feather Conglomerate.

Nevertheless, on Gondwana, glossopterid ecosystems were profoundly affected by volcanism-induced global climate change (Cui and Kump, 2015; Kaiho et al., 2020) during the Lopingian (Mays et al., 2019);

however, the timing of the demise of glossopterid forests predates the marine EPE by \sim 370 kyr (Fielding et al., 2019). The current contribution addresses several of these hypotheses, with a focus on elucidating

the state of the Lopingian terrestrial environment on Gondwana in the lead up to the EPE.

2. Stratigraphy and bio-/chronostratigraphy

This review encompasses Late Permian (Lopingian) paleosols that are preserved across multiple basins on the Panthalassic margin of Gondwana (Figs. 1 & 2). A central question addressed in this section is 'Which strata represent the Lopingian on Gondwana, and how secure are those conclusions?'. This question is addressed by compiling biostratigraphic age information, radiometric ages, lithostratigraphic correlations, and correlations of biostratigraphic schemes to the wellconstrained eastern Australian palynoassemblages (Barbolini et al., 2016). From west to east (and north to south) these basins are: 1) the Paganzo Basin of northwestern Argentina; 2) the Paraná Basin, considered here are strata exposed in southern Brazil and Uruguay; 3) the Main Karoo and Lebombo basins in South Africa; 4) the Transantarctic basins of Antarctica; and 5) the Sydney Basin of Australia (Fig. 1). The paleogeographic position of each location is determined based on the plate reconstruction of Torsvik et al. (2012) and the paleolatitude calculator of Van Hinsbergen et al. (2015). The La Golondrina Basin of southern Argentina also represents a plausible Lopingian succession, based in part on the presence of the Late Permian glossopterid ovulate structure Dictyopteridium (Archangelsky, 1992), of paralic to terrestrial strata (the La Golondrina Fm.). Systematic sedimentology and paleosol analyses, however, are lacking from this basin, and therefore are not included herein. The paleobotanical record of the La Golondrina Basin is welldescribed and suitable for integration into a systems science style analysis of the Late Permian (Archangelsky and Cúneo, 2002; Cariglino, 2013, 2018). These basins are bordered by uplifted blocks and terranes that undoubtedly figured prominently in the arrangement of soils, flora, and fauna on these paleolandscapes. However, these were inherently non-subsiding regions and thus do not have a high preservation potential, however, we encourage further study to reveal potential archives of Lopingian strata and sedimentary systems from these regions. From west to east these uplifted regions are: 1) the Pampean Arch; 2) the Asunción Arch; 3) the Río de La Plata Craton; 4) the Windhoek- and Cargonian-Highlands; and 5) an arc and foreland basin setting along the margin of the East Antarctic Craton. Paleosols discussed herein are based on, or related to, the paleosol taxonomic scheme of Mack et al. (1993) with references to modern soil systems as analogs.

2.1. Stratigraphy and geologic setting

2.1.1. Paganzo Basin

The Paganzo Basin is a late Paleozoic depocenter in northwest Argentina that was situated along the paleo-active margin of Gondwana (Limarino and Spalletti, 2006), located in modern day San Juan and La Rioja provinces. A succession of strata exists beginning in the mid-Carboniferous through the Early Permian (Limarino and Spalletti, 2006; Limarino et al., 2014), however, this region was thought to be non-subsiding prior to the deposition of the Talampaya Fm. (Spalletti, 1999), regarded as Triassic in age and recording the first of several rifting events that created the Ischigualasto-Villa Unión Basin (Spalletti, 1999; Zerfass et al., 2004). Recent radiometric dating of air fall tuffs in the upper Talampaya Fm., however, indicate that this unit is Late Permian in age, thus decreasing the duration of the unconformity between the Paganzo Group strata and the Talampaya Fm., and indicating an earlier onset of Choiyoi-related continental rifting in the region (Gulbranson et al., 2015b; Spalletti and Limarino, 2017). The Talampaya Fm. is well exposed in roadcuts and outcrops in the Bordo Atravesado area, Cuesta de Miranda, in the Sierra de Famatina (Zhang et al., 1998; Limarino and Spalletti, 2006). In this area the Talampaya Fm. records a succession of volcanic-lithic conglomerates, fluvial sandstones and overbank siltstones, eolian sandstones, and playa lake facies interbedded with volcanic ash deposits (Zhang et al., 1998; Gulbranson et al.,

2015b). Here, a new description of Protosols is made for facies association 6 of Gulbranson et al., 2015b.

2.1.2. Paraná Basin

The Paraná Basin is a massive intracratonic basin, active during the Paleozoic and Mesozoic covering modern day regions of southern Brazil, Uruguay, Paraguay, and Argentina (Holz et al., 2010). The southern Brazilian sector of the Paraná Basin records Lopingian-age strata in the Morro Pelado Member of the Rio do Rasto Fm. (Limarino et al., 2014; Francischini et al., 2018a) and in the overlying Pirambóia Fm. of the western region of Rio Grande do Sul State (Fig. 1C, Dias and Scherer, 2008; Limarino et al., 2014; Francischini et al., 2018b). The Rio do Rasto Fm. contains two stratigraphic subdivisions, the lower Serrinha Member and the overlying Morro Pelado Member (Holz et al., 2010). The Morro Pelado Member is interpreted as a succession of fluvial sandstones, overbank siltstones and mudstones, lacustrine deposits, and eolian sandstones (Holz et al., 2010; Francischini et al., 2018b), and this stratigraphic unit is exposed in the Bagé and Aceguá municipalities of Rio Grande do Sul State (Fig. 1C, Cisneros et al., 2005; Martinelli et al., 2017; Francischini et al., 2018b).

The Lopingian-age Pirambóia Fm. of the Brazilian sector of the Paraná Basin (western Rio Grande do Sul State) reflects a succession of sandstone-dominated strata interpreted as various scales of eolian facies under variable hydrologic conditions (Lavina et al., 1993; Dias and Scherer, 2008). The occurrence of regional eolian deposition is interpreted as a tectonic response to Choiyoi volcanism and the withdrawal of previous epicontinental seas (Spalletti and Limarino, 2017). The Pirambóia Fm. eolian facies are interpreted to consist primarily of sand sheet, draa (large-scale merged dunes), and interdune facies interpreted as a "wet erg" condition (Dias and Scherer, 2008), in which the ratio of sediment availability (the volume of sediment capable of being transported) to sediment supply (total amount of sediment in the sediment source area) is less than that of a "dry erg" state due to higher water table elevations acting to trap sediment (Kocurek and Fielder, 1982; Lancaster, 1992; Kocurek and Lancaster, 1999).

The Uruguayan sector of the Paraná Basin Records the last vestiges of an inland sea in the transition of the Guadalupian Yaguarí Fm. (de Santa Ana et al., 2006) to the overlying Lopingian Buena Vista Fm. (Piñeiro et al., 2007). The Yaguarí Fm. is correlative with the Serrinha Member of the Rio do Rasto Fm. to the north (Holz et al., 2010; Limarino et al., 2014). The Buena Vista Fm. is interpreted as a fluvial-alluvial-lacustrine facies association, with low-sinuosity stream systems under a semi-arid climate. This interpretation is based on the normally-graded intraformational mudstone conglomerates and the presence of carbonate nodules in red mudstone (Goso et al., 2001; Piñeiro et al., 2012).

2.1.3. Main Karoo and Lebombo basins

The Late Permian is recognized in the Main Karoo Basin as strata of the Beaufort Group, which consists of four formations arranged by their spatial distribution of outcrops and defined as being west of the 24°E meridian or east of the 24°E meridian (Fig. 1B). West of the 24°E meridian, the Teekloof Fm. represents Lopingian-age strata (Smith, 1990, 1995). East of the 24°E meridian the Balfour and Normandien fms. Document a relatively well-constrained Lopingian-Induan succession of terrestrial strata (Smith and Ward, 2001; Retallack et al., 2003; Botha and Smith, 2007; Barbolini et al., 2016; Gastaldo et al., 2014, 2020a). The Balfour Fm. is tentatively subdivided into 5 members (from oldest to youngest): Oudeberg Mbr., Daggaboersnek Mbr., Barberskrans Mbr., Elandsberg Mbr., and the Palingkloof Mbr., although the validity of the Elandsberg and Palingkloof mbrs. has been challenged (Gastaldo et al., 2021).

The Lebombo Basin occurs to the north and east of the Main Karoo Basin (Fig. 1B). In this region the Lopingian-age strata of the Emakwenzini Fm. occurs in deeply weathered outcroppings. In general, the macroflora of the Emakwenzini Fm. and similar vertical lithostratigraphic associations correlate to the Normandien Fm. of the adjacent

Main Karoo Basin (Bordy and Prevec, 2008). The Emakwenzini Fm. of the Lebombo Basin preserves a siliciclastic sandstone-coal succession of variable thickness across the area (Bordy and Prevec, 2008). Sandstones in this succession document alluvial in-channel depositional environments and overbank fine to wetland environments of two predominant facies associations: 1) a low-sinuosity fluvial system and associated lacustrine deposits; and 2) an alluvial setting with abundant overbank fine deposits and peat deposits (Bordy and Prevec, 2008).

2.1.4. Transantarctic Basin

The Late Permian in the Transantarctic Basin is represented by The Upper Member of the Buckley Fm. (central Transantarctic Mountains, CTAM), The Lower Member of the Fremouw Fm. (in the Shackleton Glacier area), and the upper portion of the Weller Coal Measures in southern Victoria Land (SVL) (Figs. 1E & & 2, Barrett et al., 1986; Collinson et al., 2006). These strata were deposited in a retroarc foreland basin (Dalziel and Elliot, 1982; Collinson, 1990), approximately 1500 km south of the Karoo and Lebombo basins, which displayed prominent volcanic activity during the Lopingian in the vicinity of the present-day Shackleton Glacier area (Pankhurst, 2002; Elliot et al., 2017). The Upper Member of the Buckley Fm. is a suite of volcaniclastic and fossiliferous sandstones, coal and minor amounts of siltstone. The Buckley Fm. is overlain by the Fremouw Fm. in the CTAM area. The Fremouw Fm. represents a change in composition to more quartzose sandstone and an increased abundance of variegated siltstones interspersed between multistory sandstones (Barrett, 1969; La Prade, 1982; Retallack and Krull, 1999; Krull and Retallack, 2000). The Fremouw Fm. and Buckley Fm. contact is likely diachronous, however, the Lower Member of the Fremouw Fm. in the Shackleton Glacier area contains characteristic Permian macroflora.

The Weller Coal Measures of SVL are subarkosic in composition, reflecting deposition in a structurally-defined sub-basin (Collinson et al., 1994). This unit contains a suite of fossiliferous sandstone, coal, and siltstone overlain by the Feather Conglomerate, a prominent cliff-forming arrangement of quartzose sandstone. The Upper Member of the Buckley Fm., the Lower Member of the Fremouw Fm., The Weller Coal Measures, and the Feather Conglomerate have been interpreted as reflecting low-sinuosity stream systems, draining towards the Sydney Basin (Barrett, 1969; Collinson et al., 1987; Isbell, 1991).

2.1.5. Sydney and Bowen basins

Deposition of sediment during the Late Permian in the Sydney and Bowen basins took place in a foreland basin setting with an adjacent volcanic arc (Wachbuscha et al., 2009; Metcalfe, 2013), which was part of a convergent plate boundary along the Australia-Tasmania-Antarctica margin of Gondwana (Metcalfe et al., 2015; Elliot et al., 2017). Lopingian strata of the Sydney and Bowen basins yields the highest-resolution stratigraphy from the detailed palynostratigraphy and high-precision U-Pb geochronology (Mundil et al., 2006; Metcalfe et al., 2015; Barbolini et al., 2016). Lopingian strata ocurs as the Illawarra Coal Measures, the Newcastle Coal Measures, and the Wittingham Coal Measures (Fig. 2). The Bowen Basin records a similar succession of strata as the Black Alley Shale and Bandanna Fm (Mundil et al., 2006). The lowermost part of the Illawarra Coal Measures records the final phase, "P4", of glaciation on Gondwana during the Late Paleozoic (Fielding et al., 2008). Multiple sub-divisions of these coal measures have been proposed across each basin, reflecting long-standing interest in organizing the coal-bearing strata in this region. However, most notable among these subdivisions are those units that have recently provided highly precise and stratigraphically consistent radiometric ages. These include: 1) the Permian-Triassic boundary at the base of the Coal Cliff Sandstone (Narrabeen Group) (Fielding et al., 2019); 2) the Changhsingian Bulli Coal of the Illawarra Coal Measures (Metcalfe et al., 2015); 3) the early Changhsingian Farmborough Claystone of the Illawarra Coal Measures (Metcalfe et al., 2015); and 4) the Wuchiapingian-Changhsingian Adamstown and Boolaroo fms. of the Newcastle Coal Measures

(Metcalfe et al., 2015). A wide range of paleoenvironments are interpreted from the Sydney and Bowen basins (Herbert, 1997; Fielding and Alexander, 2001), but reflect a general falling stage sea-level tract and progradational succession of fluvial, deltaic, and coastal plain facies during the Lopingian (Fielding et al., 2019).

2.2. Bio-/chronostratigraphy

The stratigraphic schemes presented below attempt to synthesize a broad cross-section of geochronologic and biostratigraphic work aimed at refining the ages of strata that may, or may not, be Late Permian in age. The Late Permian was ~8 million years in duration, thus, this synthesis seeks to describe the modes of paleoenvironment and paleoclimate across Gondwana during the Late Permian, while also discussing the nuanced spatial and temporal variation in paleoenvironment and paleoclimate deduced in the study regions. In many cases, controversy exists around the placement of the Permian-Triassic boundary relative to the extinction interval in a given succession of strata (cf. Retallack et al., 2003; Collinson et al., 2006; Gastaldo et al., 2009; Modesto and Botha-Brink, 2010; Piñeiro et al., 2012; Lanci et al., 2013; Ernesto et al., 2020; Gastaldo et al., 2020b, 2021), as narrowing the scope of chronostratigraphic resolution can result in profound impacts on the relationships of vertebrate, invertebrate, and plant taxa around the end-Permian mass extinction. Notably, the revision of the timing and significance of the Daptocephalus-Lystrosaurus Assemblage Zone in the Karoo Basin as being older than the marine-defined EPE and with Lystrosaurus not representative of a "disaster taxon" (Gastaldo et al., 2019; Modesto, 2020). Perhaps more important than controversy is the likelihood of diachroneity related to floral and faunal provincialism across Gondwana (Barbolini et al., 2016). This likelihood hampers correlations of biostratigraphy between depositional basins on Gondwana, but may also hold crucial clues on phytogeographic variation across Gondwana in the face of paleoenvironmental change (cf. Smith, 1995; Ward et al., 2000). Continued work on refining the numeric geologic timescale and age ranges of first appearance datums is of the utmost importance. The scope of this review, however, is broad to reflect Lopingian soil-forming environments in general. Therefore, stratigraphic units that contain multiple lines of independent evidence of being at least, in part or within uncertainty, Lopingian in age are used in this analysis.

2.2.1. Paganzo Basin

The Talampaya Formation was previously assigned as the basal unit of the Triassic succession of the Ischigualasto-Villa Unión rift basin (Romer and Jensen, 1966), based on lithostratigraphy in the absence of biostratigraphic age information at the time. Diverse trace fossil records from the Talampaya Fm., however, have Permian affinities (Zhang et al., 1998). Recent U-Pb CA-ID-TIMS dating of zircons extracted from airfall tuffs within the uppermost succession of playa lake facies of the Talampaya Fm. at the Bordo Atravesado locality yields an age of 252.38 + 0.09/-0.22 Ma (Changhsingian) (Gulbranson et al., 2015b). These results place the conformable lower sections of the Talampaya Fm. in the Late Permian, as well. However, the basal contact of this unit is undefined in terms of stratigraphic age (Fig. 2). The revised age model for the Talampaya Fm. indicates that continental rifting associated with the later stages of the Choiyoi volcanic system occurred during the Lopingian, reflecting a transition between the earlier Paganzo Basin foreland system and the younger Ischigualasto-Villa Unión Basin rift system (Spalletti and Limarino, 2017).

2.2.2. Paraná Basin

The Brazilian sector of the Paraná Basin hosts an unconformable succession of Lopingian strata including the Morro Pelado Member of the Rio do Rasto Fm. and the overlying Pirambóia Fm. The Rio do Rasto Fm. represents Guadalupian through Lopingian strata divided into two members: the Serrinha Member, and the overlying Morro Pelado

Member. The Serrinha Mbr. yields: a provisional U—Pb LA-ICPMS age of 270.61 + 1.76/-3.27 Ma (Francischini et al., 2018a); palynological assemblages correlated to the Kungurian-Wordian Luekisporites virkkiae Zone (Neregato et al., 2008); bivalve associations with the Guadalupian (Simões et al., 2017); and plant macrofossil assemblages correlated to the Wordian Sphenophylluum paranaensis Zone (Rohn and Rösler, 2000). The overlying Morro Pelado Mbr. preserves vertebrate assemblages assigned to the Tapinocephalus Assemblage Zone of the Main Karoo Basin (Malabarba et al., 2003; Dias-da-Silva, 2012), which would indicate a contradictory Guadalupian age for the Morro Pelado Member if this Assemblage Zone was synchronous across Gondwana. Temnospondyls occur in the Morro Pelado Mbr., consistent with a Middle-Late Permian age especially considering possible migration routes from Pangaea (Pacheco et al., 2016). The Morro Pelado Mbr., therefore, is Guadalupian-early Lopingian age on the basis of the better constrained underlying Serrinha Mbr., but further investigations need to be undertaken to confirm the age and age range of this unit.

The Pirambóia Fm. in the western portion of the Rio Grande do Sul State should be noted as being distinct from a formation with an identical name to the east in Rio Grande do Sul State and São Paulo State (Fig. 1C, Reis et al., 2019; Soares et al., 2008). The eastern unit contains a succession of eolianites with stratigraphic contacts with Triassic and Jurassic strata and a Mesozoic assemblage of conchostracans and ostracods (Soares et al., 2008). Thus, the Pirambóia Fm in the western sector of the Rio Grande do Sul state represents a Lopingian-Induan age range based on the stratigraphic contacts with the underlying, Lopingian-age (Fig. 2), Morro Pelado Mbr. (Rio do Rasto Fm.); and the overlying Induan-age Sanga do Cabral Fm. Although imprecise for age determination, the Pirambóia Fm. does contain the Chelichnus and Dicynodontipus ichnofacies, consistent with a dicynodont trace maker (Francischini et al., 2018b). Considering the refinement in age of the overlying Sanga do Cabral Fm. (Abdala et al., 2002), the age range of the Pirambóia Fm. in the western area of Rio Grande do Sul State must be no younger than the Induan (The Pirambóia Fm. in eastern Rio Grande do Sul and São Paulo states is likely Triassic-Jurassic in age).

The Uruguayan sector of the Paraná Basin Records the last vestiges of an inland sea in the transition of the early Guadalupian Yaguarí Fm. (269.8 ± 4.7 Ma, de Santa Ana et al., 2006) to fully terrestrial strata of the overlying Buena Vista Fm. The age range of the Buena Vista Fm. is controversial and may extend from the Guadalupian across the Permian–Triassic boundary (Piñeiro et al., 2012) or the unit may be restricted to the Lopingian (Holz et al., 2010). Recent attempts to refine the chronostratigraphy of the Buena Vista Fm. in the Uruguayan sector of the Paraná Basin utilize magnetostratigraphy and vertebrate fossil associations to place this unit in the Lopingian (Ernesto et al., 2020). Nevertheless, a Lopingian-age for at least the upper member of the Buena Vista Fm., in general, is consistent with these numerous stratigraphic and paleobiologic analyses (Piñeiro et al., 2012).

2.2.3. Main Karoo and Lebombo basins

Lopingian-age strata in the Main Karoo Basin are defined primarily on the basis of vertebrate biostratigraphy (Smith and Ward, 2001; Smith and Botha, 2005; Botha and Smith, 2007). The transition from the Daptocephalus Assemblage Zone to the Lystrosaurus Assemblage Zone has been long-held to be synchronous with the EPE described from marine deposits in China. However, a recent U-Pb CA-ID-TIMS age of 252.24 \pm 0.11 Ma indicates that the boundary between these Assemblage Zones, as currently defined, is ∼1 Ma older than the marine-defined EPE (Gastaldo et al., 2020b), consistent with palynologic results from this Assemblage Zone (Barbolini et al., 2018). Furthermore, the Lystrosaurus Assemblage Zone fails to meet the criteria of a so-called "disaster taxon" (Modesto, 2020), further separating the origination of these taxa from a connection to the EPE. Radiometric dating of zircons, however, serves to calibrate many of the stratigraphic units in this area, permitting an accurate correlation with the established eastern Australian palynoassemblages for further age refinement (Barbolini et al., 2016;

Fielding et al., 2019; Gastaldo et al., 2021). The Teekloof Fm. is a Guadalupian-Wuchiapingian age unit to the west of the 24°E meridian and contains a radiometric age of 260.62 \pm 0.081 Ma (Day et al., 2015). To the east of the 24°E meridian, the Middleton and overlying Balfour fms. Are recognized; and further to the north in the Main Karoo Basin the Normandien Fm. is recognized as correlative to a portion of the Balfour Fm. The Middleton Fm. represents the Guadalupian through Wuchiapingian age strata, bracketed by two radiometric ages of 259.26 \pm 0.060 Ma (for the Rubidge et al., 2013 ages, the uncertainty reported here is only the analytical uncertainty) and 256.25 \pm 0.092 Ma (Rubidge et al., 2013). The Balfour Fm. consists of five subdivisions: Oudeberg Member, Daggaboersnek Member, Barberskrans Member, Elandsberg Member, and the Permian-Triassic Palingkloof Member. Two radiometric ages bracket the strata of the Balfour Fm. with an age of <255.2 Ma for the Daggaboersnek M. (Rubidge et al., 2013), and an age of 253.48 \pm 0.15 Ma for the Elandsberg M. (Gastaldo et al., 2015). The Normandien Fm. is constrained by the Clouston Farm palynoassemblage (Prevec et al., 2010), which is correlated to the APP5 biozone (Wuchiapingian-Changhsingian) of eastern Australia (Barbolini et al., 2016). A provisional Late Permian interpretation of U—Pb ages on zircons suggested a dramatic shift of the Late Permian time to the Lower Beaufort Group (Fildani et al., 2007, 2009); however, these interpretations have been challenged recently by revised zircon geochronology and magnetostratigraphy of the Lower Beaufort Group that suggests a Guadalupian age (Lanci et al., 2013). A Guadalupian age for the unit is consistent with the aforementioned vertebrate, pollen/spore, and macroflora biostratigraphy; and numerous radiometric age constraints for the Upper Beaufort Group.

The Emakwenzini Fm. of the Lebombo Basin is assigned to the Lopingian on the basis of lithostratigraphic correlations with the Normandien Fm. of the Main Karoo Basin (Fig. 2), and correlations of well-preserved floras. The distinct Late Permian glossopterid fructification *Dictyopteridium* preserved in the Emakwenzini Fm. is correlative with adjacent Lopingian strata in the Main Karoo Basin (Bordy and Prevec, 2008; Prevec et al., 2009). Moreover, a distinctly Lopingian insect fossil association of grylloblattids occurs in the Emakwenzini Fm. (Aristov et al., 2009). However, the upper contact of the Emakwenzini Fm. is disconformable. Therefore, despite the aforementioned correlations, significant uncertainty exists about the age range of this stratigraphic unit

2.2.4. Transantarctic Basin

The Upper Permian in the Transantarctic Basin is represented by the Upper Member of the Buckley Fm. (CTAM), the Lower Member of the Fremouw Fm. (Shackleton Glacier area, CTAM), and the upper portion of the Weller Coal Measures (SVL) (Collinson et al., 2006). At Graphite Peak and Mt. Achernar in the CTAM, Protohaploxypinus microcorpus occurs below the contact of the Buckley and Fremouw fms. (Fig. 1E, Collinson et al., 2006). The P. microcorpus biozone may indicate an Early Triassic age for part of the Upper Member of the Buckley Fm. based on the APP6 biozone of Australia (Mays et al., 2019) if it can be assumed that this biozone was not diachronous across Gondwana. However, detrital zircon U-Pb LA-ICPMS ages for the Upper Member of the Buckley Fm. yield maximum depositional ages (not accounting for the possibility of Pb-loss) of 253.5 \pm 2.0 Ma (Elliot et al., 2017), confirming a Changhsingian age. The overlying Upper Member of the Fremouw Fm. (CTAM) yields Cynognathus remains correlated to the Cynognathus-Cricodon-Ufudocyclops biozone of the Karoo Basin suggesting a late Anisian-Landinian age (Sidor et al., 2014; Hancox et al., 2020), and thus constraining the Middle and Lower mbrs. of the Fremouw Fm. to the Early and early Middle Triassic. The diachroneity of the Fremouw Fm. and Buckley Fm. contact is suggested based on: 1) volcaniclastic composition of the Lower Fremouw Fm. in the Shackleton Glacier area; 2) the occurrence of glossopterid fossils in the Lower Fremouw Fm.; and 3) Lystrosaurus remains a few meters above the last glossopterid fossil occurrence at Collinson Ridge (Collinson et al., 2006). Thus, in the

Shackleton Glacier area the Lower Fremouw Fm. is in part, Lopingian in age and likely extends into the Induan.

The Weller Coal Measures yield palynoflora related to the Protohaploxypinus biozone and Praecolpatites sinuosus (Kyle and Schopf, 1982; Farabee et al., 1990; Askin, 1995). While the Protohaploxypinus biozone correlates to the latest Carboniferous-Early Permian (Cisuralian) APL4-APP1 Australian biozone (Laurie et al., 2016), the P. sinuosus fossils indicate a Cisuralian-Guadalupian age. The overlying Feather Conglomerate has not yielded significant microfossil or macrofossils for biostratigraphic correlation (Fig. 2); however, the Lashly Fm. (overlying the Feather Conglomerate) yields palynomorphs of the Alisporites biozone, indicating an Early Triassic age for the Lashly A Member (Kyle and Schopf, 1982). While not well-constrained in terms of palynology, and an absence of radiometric ages, the available biostratigraphic information of the Weller Coal Measures and of the overlying Lashly Fm. indicate an age range extending from the Early Permian to Late Permian given the suggested conformable contact of the upper Weller Coal Measures with the Feather Conglomerate, and of the Feather Conglomerate and the Lashly Fm. (Retallack and Krull, 1999; Tewari et al., 2015).

2.2.5. Sydney and Bowen basins

Updated U—Pb CA-ID-TIMS ages for the Sydney Basin are used herein (Metcalfe et al., 2015; Fielding et al., 2019), and consist of the addition of twenty-eight ages reported in Metcalfe et al., 2015 and a single age from Fielding et al., 2019. For the northern Sydney Basin the Wittingham Coal Measures through the Adamstown Fm. of the Newcastle Coal Measures are Wuchiapingian in age (3 U-Pb ages); whereas the remainder of the Newcastle Coal Measures up to the contact with the overlying Narrabeen Group (10 U-Pb ages) are Changhsingian in age (Metcalfe et al., 2015). For the southern Sydney Basin, a portion of the Illawarra Coal Measures (the Woonona Coal through the Kembla Sandstone) are Wuchiapingian in age (2 U-Pb ages); whereas the Wongawilli Coal through the Scarborough Sandstone may be Changhsingian (3 U-Pb ages) in age (Metcalfe et al., 2015). However, a single U—Pb age from Fielding et al. (2019) suggests the base of the Coal Cliff Sandstone may mark the Permian-Triassic boundary.

The Bowen Basin contains the Tinowan Fm., Black Alley Shale, and Bandanna Fm. as Upper Permian units. The Tinowan Fm. is Wuchiapingian in age based on two U—Pb ages (Metcalfe et al., 2015). The Black Alley Shale crosses the Wuchiapingian-Changhsingian boundary based on the results of two U—Pb ages (Metcalfe et al., 2015). The Bandanna Fm. has been dated to the Changhsingian based on 5 U-Pb ages (Mundil et al., 2006; Metcalfe et al., 2015).

3. Soil systems across the panthalassic margin of Gondwana

Similar to modern soil classification schemes, we consider here the broad subdivision of soils into two categories: 1) mineral soils, which are composed primarily of non-organic soil horizons, but can include some O horizon development; and 2) organic soils, which are composed primarily of vertically stacked O horizons, in which the organic material consists of a range of plant organs in addition to microbial biomass components. Organic soils are primarily preserved in the stratigraphic record as coal, thus the areal extent and paleolatitudes of coal-bearing strata is of interest in this review. From these two categories, mineral paleosols are further organized by recognition of subsoil horizons (B horizons) that are genetically related to an ensemble of distinct soilforming processes (e.g., illuviation of clay; conspicuous soil-formed minerals, podzolization; calcification; prolonged oxidation/reduction reactions; etc.) (e.g., Retallack, 1988; Mack et al., 1993; Tabor et al., 2017). Analogs to extant soils are often made in paleosol studies. However, we recognize that many factors used in modern classification schemes are not capable of being measured in paleosols. Such factors rely on interpretation of varying amounts of certainty. These include: soil solution pH (Lukens et al., 2018); cation exchange capacity and base

saturation (Nordt et al., 2011); exchangeable sodium percentage (Sheldon and Tabor, 2009); monthly/annual temperature and precipitation trends (Sheldon et al., 2002; Nordt and Driese, 2010; Gulbranson et al., 2011; Gallagher and Sheldon, 2013). Modern soil analogs, however, are crucial for developing a systematic understanding of soil-forming processes and their relative history within a given paleosol profile.

Climate is an integral part of the soil system. However, climate is inherently interpretive when derived from paleosols, and here is evaluated in the context of the support provided for a given interpretation by the data that are available. Moreover, paleosol-based paleoclimate reconstructions are susceptible to wide-ranging interpretations when paleosol profiles are used to reconstruct paleoclimate through time, Thus, careful experimental design and sampling in comparing contemporaneous paleosols or paleo-catenas is a vital screening tool to avoid erroneous paleoclimate inferences (see Dzombak et al., this volume). Sedimentary systems in each depositional basin are summarized, focusing on sediment transport directions and sediment compositions, with special emphasis on likely vectors for wind-blown sediment transport (e.g., the Rio do Rasto and Pirambóia fms. of the Paraná Basin). The paleobiology of primary producers and fauna in each depositional basin is discussed in terms of diversity of these paleoecosystems. The geochemistry of these paleosols is also be presented as an archive of potentially multiple processes acting on these soils: 1) weathering; 2) parent material composition; 3) rates of sedimentation versus pedogenesis (sensu Kraus and Aslan, 1993; Kraus, 1999; Gastaldo et al., 2014); and 4) potential correlations with biotic diversity.

3.1.1. Paganzo Basin

Protosols are the principal paleosol recognized in the Talampaya Fm. Here we systematically describe the Protosol paleosol profiles and their stratigraphic association. Profile development in these Protosols is minimal and reflect the observations of coarse angular blocky soil structure development, destruction of primary sedimentary fabric, and slight redoximorphic character (Fig. 3A; 4). Horizons observed in these Protosols include Bw and C horizons with erosional and deformed contacts between Bw horizons and an overlying C horizon (Fig. 3A). Bw horizons are >30 cm thick, display a coarsening downward trend in angular block soil structure, and display redoximorphic colors in the upper 10 cm of the horizons, with sparse mottling in the lower 2/3 of the horizon. C horizons are 10-20 cm thick, massive to crudely bedded and display coplanar zones of redoximorphic color. Unique features indicating the subaerial weathering of parent material (Fig. 3B) occur as outsized clasts of igneous and metamorphic rocks. Conglomeratic parent material within a pebbly lithic arkosic arenite contains clasts of the nearby Ordovician Nuñorco granite that was decomposed to grus (Fig. 3B). The grus, however, is in situ, indicating very low flow competence and shear stress for the transport and erosion of this material. These paleosols are interbedded between lacustrine deposits interpreted to reflect playa lake conditions in the upper portion of the Talampaya Fm., as well as interbedded between sandsheet and dune facies of the eolian succession lower in the formation (Facies Associations 7 and 6 of Gulbranson et al., 2015b). Protosol profiles in the Talampaya Fm., are overly thickened cumulative profiles (Figs. 3A, 4). Therefore, these Protosols represent a soil-forming environment where the rate of pedogenic modification was nearly equivalent to the rate of deposition. Additionally, the locus of sedimentation, at the locations where these paleosols are observed shifted laterally over time, giving rise to solitary cumulative profiles of Protosols separated by nonpaleosol material.

3.1.2. Paraná Basin

Protosols occur in the Buena Vista Fm. of the Uruguyan sector of the

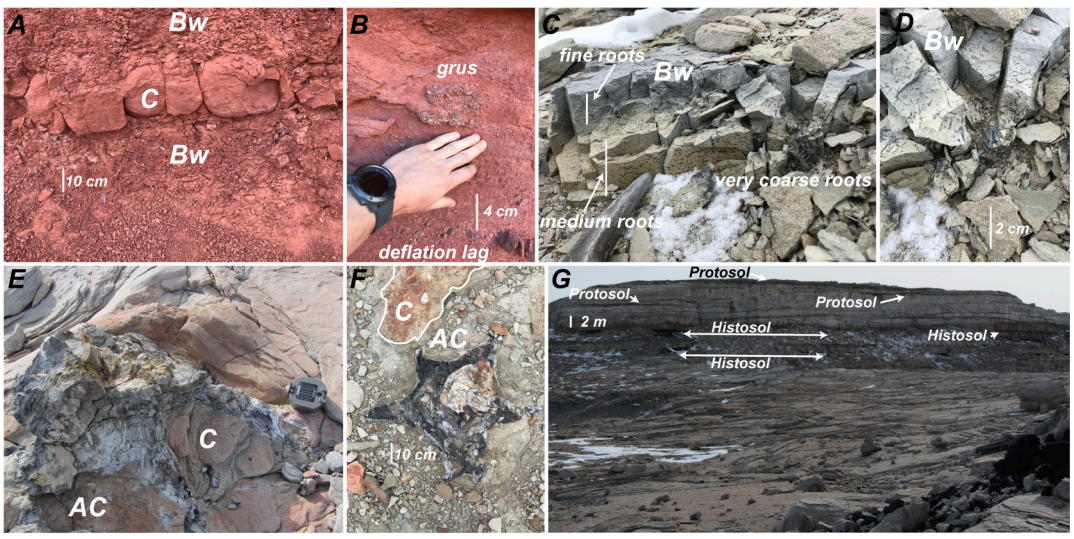


Figure 3.

Fig. 3. Field photographs of paleosols in the study region. A and B are for the Paganzo Basin, C-G are for the Transantarctic Basin. A) Cumulative Protosols in the Talampaya Fm., displaying at least 50 cm of Bw horizon thickness with partially modified C horizon sandstone separating distinct paleosol profiles. Basal contact of the C horizon sedimentary deposit is undulatory, but does not truncate underlying paleosol material. Bw horizons display development of coarse-medium subangular blocky structure and slight redoximorphic variation in color. B) Examples of the weathering environment of the Talampaya Fm., granitic grus in a pebbly arkose arenite. Deflation lags are inferred from coplanar associations of pebble-cobble angular lithic fragments. C) Solitary Protosol profile, Lower Fremouw Fm., Shenk Peak (CTAM). A wide range of permineralized roots and rootlets are preserved in this Protosol. Roots are interpreted to reflect the rooting habits of glossopterids based on the clear Vertebraria anatomy of the coarse and very coarse permineralized roots. Fine roots are predominant in the upper light gray portion of the Bw horizon, and medium-very coarse roots occur in the lower yellow-brown Bw horizon, with the coarsest roots occurring in both divisions of the Bw horizon. D) Topdown aspect of C, displaying the clear Vertebraria anatomy of the very coarse roots. E and F) solitary in-channel sand-rich Protosols. E) In-channel solitary Protosol developed on a macroform top in the Weller Coal Measures, Allan Hills with in situ glossopterid trunk. Modification of the uppermost horizon by fine roots has destroyed some sedimentary structures giving rise to the thin AC horizon. F) top-down aspect of a solitary Protosol with in situ glossopterid trunk at Collinson Ridge, Lower Fremouw Fm., displaying limited modification of the volcanic-lithic arenite near the prominent roots. G) Associations of mineral and organic paleosols in the upper Weller Coal Measures and overlying Feather Conglomerate, Allan Hills. The foreground exposed bedding planes detail several accumulations of macroform elements and the in-channel forest described in Gulbranson et al. (2020). The background of the image shows the association of overlying laterally continuous Histosols grading into thin laterally discontinuous Histosols near the contact with the Feather Conglomerate. The Feather Conglomerate is the prominent ridgeforming sandstone and contains several stratigraphic positions of laterally discontinuous Protosols (Delores pedotype) representing localized channel abandonment, and capped by a laterally continuous Protosol (Delores pedotype) indicating avulsion of the low-sinuosity system from this area. (For interpretation of the references to color in this figure legend, the reader is referred to the web version of this article.)

Paraná Basin (Piñeiro et al., 2012; Ernesto et al., 2020). The Protosols of the Buena Vista Fm. are ~50 cm thick, interbedded in a succession of fluvial sandstones and conglomerates, the latter yielding abundant temnospondyl remains (Colonia Orozco fauna; Piñeiro et al., 2012), and display a uniform reddish-brown color. The fluvial sandstone and conglomerate units occur as discrete elements in the same facies, which is a fining upward low-sinuosity fluvial-alluvial system, with four fining upward trends recognized (Ernesto et al., 2020). The transition from transport of conglomerate, including re-working of debris such as temnospondyl bones, to sand indicates rapidly waning flow regimes typical of ephemeral fluvial systems (Ernesto et al., 2020). Mudstone intraformational clasts are abundant throughout the Buena Vista Fm. indicating the prevalence of degradational fluvial systems on eroding Protosol material on the paleo floodplain. Therefore, a composite to compound profile type is likely for the Buenva Vista Fm. Protosols.

3.1.3. Main Karoo and Lebombo basins

This review of the Karoo and Lebombo Basins covers a distance of approximately 1000 km and an area of $\sim\!300,\!000$ km². In spite of this, the preservation and quality of outcrop exposures (i.e., not dissected by numerous faults) is limited to a handful of well-studied outcrop areas (Pace et al., 2009; Gastaldo et al., 2009). Paleosols in the Main Karoo Basin have been described from the Teekloof Fm. (Smith, 1990, 1995), west of 24°E ; and from the intensely studied Balfour Fm. (Elandsberg and Palingkloof mbrs.), east of 24°E (Table 1). The paleosols considered herein are principally mineral paleosol types, although the distribution of B horizon types and interpretations on pedogenesis are exceptionally

variable throughout this basin. Moreover, there exists a sampling bias towards paleosols east of $24^{\circ}E$, as no further study or replication of more limited results west of $24^{\circ}E$ (e.g., Smith, 1990, 1995) has occurred.

The Teekloof Fm. is correlative to the Midldleton Fm. and Oudeberg and Daggaboersnek mbrs. of the Balfour Fm. (Viglietti et al., 2017). Within the Balfour Fm. the New Wapadsberg Pass locality corresponds to the Elandsberg Mbr. (Gastaldo et al., 2020a, 2020b, 2020c) and the overlying Palingkloof Mbr. (Gastaldo et al., 2014). The Palingkloof Mbr. has been studied in the Lootsberg Pass area (\sim 7 km from New Wapadsberg Pass) and Bethulie area (\sim 150 km from Lootsberg Pass) (Retallack et al., 2003; Ward et al., 2005; Smith and Botha, 2005; Gastaldo et al., 2009).

The following discussion proceeds from oldest to youngest for the succession of paleosols and from west–east across the Main Karoo Basin. The Teekloof Fm. paleosols consist of calcic Protosols, Vertisols, and possibly Gypsisols in high-sinuosity fluvial environments of the southwestern Karoo Basin (Smith, 1990, 1995). These paleosols are interpreted to form a continuum along paleolandscapes, representing a catena-type relationship of variable drainage in an altogether intensely arid climate that led to the development of pedogenic gypsum (observed as quartz pseudomorphs after gypsum) (Smith, 1990; Retallack, 2005, Fig. 4). The mobility versus accumulation and complexation of Ca²⁺ in the paleo-soil forming environment is an intriguing problem in this succession of paleosols, especially in terms of landscape development. This is because argillic horizons that would later form vertic properties generally develop following a period of Ca²⁺ eluviation (Smith and Wilding, 1972; Khormali et al., 2003; Gunal and Ransom,

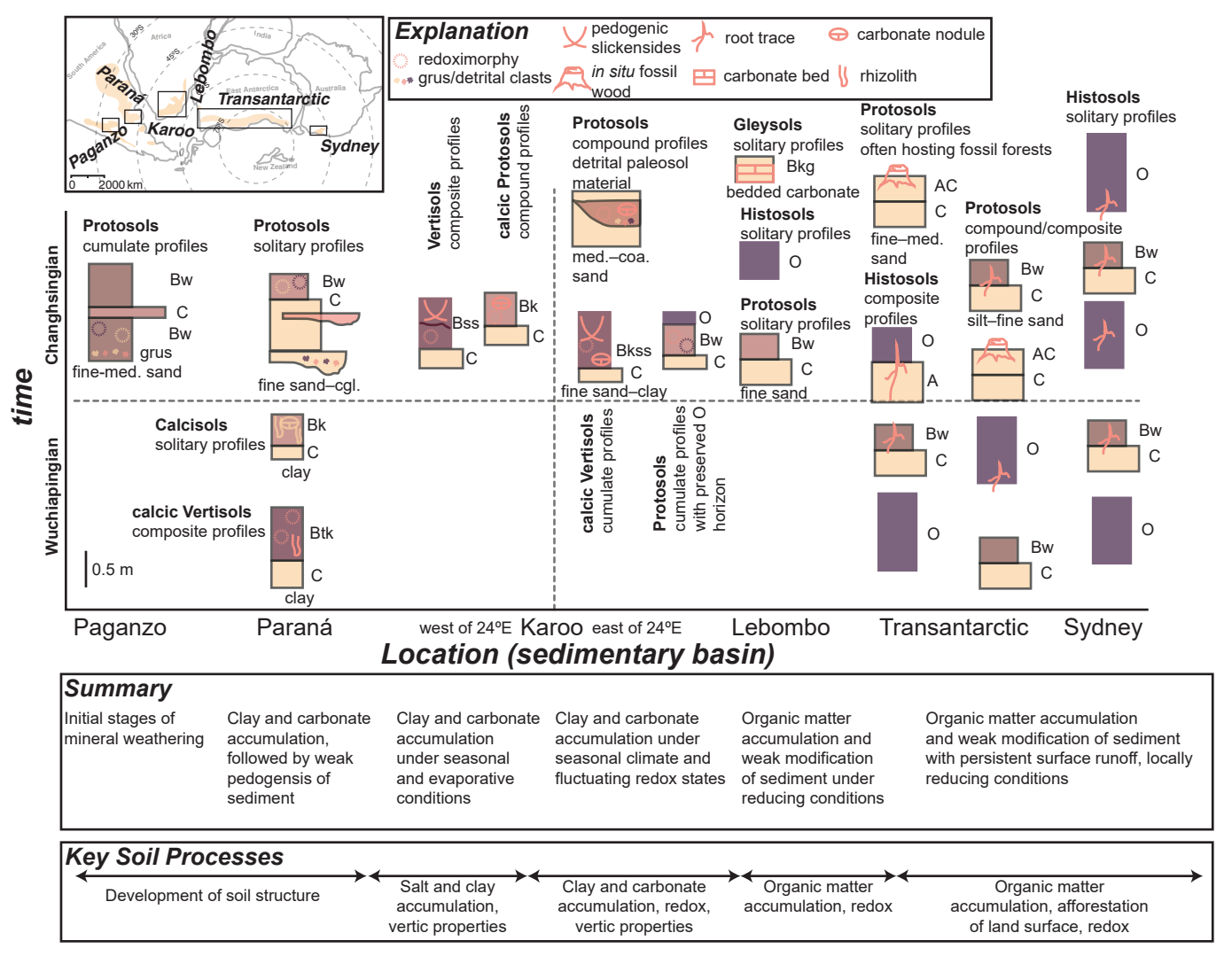


Fig. 4. Paleosol morphologies through space and time. Paleosol morphologies are summarized from the text here by sedimentary basin (x-axis) and time, reflecting Wuchiapingian vs. Changhsingian (y-axis). The inset diagram displays the study region, highlighting the location of each basin. Key paleosol profile types are annotated, however, for the Transantarctic and Sydney basins. Only key profiles are annotated and the remainder are used to illustrate the continuity of those profiles through time. Stratigraphic ordering is relative on this diagram, and does not reflect the true stratigraphic complexity of vertical and lateral associations of paleosols across this broad region. A brief summary of key soil-forming observations is provided beneath the figure, as well as a brief list of prominent soil morphologic differences that are observed in each area.

2006), and are further developed by Na⁺-driven dispersion of clay in the solum. Often carbonates will accumulate in dryland environments following argillic horizon development and the attendant changes in soil hydrology (Gile and Grossman, 1968; Pal et al., 2003; Muhs, 2007).

A succession of calcic Vertisols occurs in the lower portion of Lopingian strata in the Wapadsberg Pass area, east of 24°E (Gastaldo et al., 2020a, Fig. 4). In addition to the development of subsurface argillic horizons with vertic properties and pedogenic calcite, abundant pyrite occurs in these paleosols. The occurrence of pyrite, and the trace fossil Kathergia (Gastaldo and Rolerson, 2008), led Gastaldo et al. (2020a) to interpret these soil-forming conditions as a vertical succession of paleosols indicating variable drainage conditions and sedimentation rates. These paleosol profiles are thus interpreted as either compound or composite soil profiles depending upon the severity of base-level fall and landscape degradation in the area. A suggested sequence of pedogenic chronofacies is used to explain these paleosol morphologies: overbank deposition; drainage shift and Bw horizon formation; degradation; drainage shift and leaching leading to argillic horizon; culminating in carbonate development and associated vertic properties of the argillic horizon. The redox environment of these soils indicates that sulfur was an important source for redox reactions in these soils (cf. to the carbonate-after-siderite deposits of the Lebombo Basin) (Gastaldo et al., 2020a).

The Palingkloof Mbr. Protosols of the Karoo Basin preserve evidence Protosols in vertical association that preserve carbonate nodules or enhanced organic tissue preservation (Prevec et al., 2010, Fig. 4). The change of pedogenic carbonate development to paleosols where abundant fossil plant remains are preserved is interpreted to reflect changes in base-level and burial of the organic-rich paleosols within the phreatic zone (Gastaldo and Demko, 2011; Gastaldo et al., 2014), as these paleosols developed in an environment proximal to the paleoshoreline of small lacustrine systems. The subsurface accumulation of organic matter in weakly developed soils is one of the more common processes affecting the Entisols in the modern (McDaniel and Graham, 1992), Fluvents in particular (Lindbo, 1997), and these organic carbon-enriched horizons are usually driven by intense root action in the subsurface. In contrast, the organic-rich horizon development in Protosols of the Palingkloof Mbr. are composed of well-preserved leaf macrofossils (Prevec et al., 2010), indicating that these horizons represent burial of previous land surfaces. Compared to the underlying sequence of calcic Vertisols, these

Protosols likely formed under an aggradational deposition setting, i.e., cumulative paleosol profiles. At the Carleton Heights area (30 km NW of Wapadsberg Pass), the Palingkloof Mbr. sedimentary system contains more evidence of landscape degradation as cut-and-fill fluvial architecture, particularly in the Bethulie area. A sequence of well-developed calcic Vertisol profiles overlying the Protosols contain pedogenic nodules with internally preserved rooting structures and stable carbon isotope values consistent with well-drained open-system pedogenic calcite precipitation (Gastaldo et al., 2020a, 2020c). Localized inchannel fill deposits of a lenticular cut-and-fill deposit (Gastaldo et al., 2009), contain erosional remnants of pedogenic carbonate (interpreted as marking the Permian-Triassic boundary, Retallack et al., 2003; Retallack, 2021). Paleosols described in the Bethulie area include calcic Protosols, Calcisols, and Protosols (Retallack et al., 2003), however, the criteria for distinguishing each of these paleosols was called into question by Gastaldo et al. (2014). Gastaldo et al. (2009) interpreted this succession of strata as a high-sinuosity fluvial-floodplain system prone to avulsion episodes, with degradational landscapes and well-drained soil conditions being inferred (Gastaldo et al., 2020c), possibly due to tectonism (Viglietti et al., 2017). Soil drainage conditions, however, are interpreted to have been variable across the Karoo Basin (Tabor et al., 2007; Gastaldo et al., 2014), where the exact controls on soil drainage differences are not well-understood. The indicators for poor soil drainage versus well soil drainage derive from inferences from stable carbon isotopes of carbonate carbon and organic carbon and from Katbergia trace fossils. The timing and duration of a particular soil drainage environment was likewise variable, as polygenetic compound or composite soil profiles, gleyed calcic Vertisols, are known from the Karoo Basin (Gastaldo et al., 2020c). Indeed, the morphology of these soil profiles has been attributed to a chronofacies of soil-forming processes, wherein the vertic properties developed last following the leaching of calcium from the subsoil, development of an argillic horizon, and alteration of soil hydrology by the argillic horizon creating vertic properties (Gastaldo et al., 2020c). Coeval sedimentary strata support these interpretations of more well-drained conditions contemporaneous with landscape incision, followed by increasingly poor soil-drainage during landscape aggradation (sensu Gastaldo and Demko, 2011).

The interpretation of aridification affecting the Palingkloof Mbr. (Retallack et al., 2003; Smith and Botha-Brink, 2014), however, seems premature as the nature carbonate development in some soils but not others indicates that other causes of pedogenic carbonate development may have occurred in these paleoenvironments. Additional factors such as: dust deposition (and an understanding of eolian sediment transport and source areas); or hydrologic-enrichment of Ca²⁺ in shallow groundwaters (Gile and Grossman, 1968) could have been important in the spatially heterogeneous development of pedogenic carbonate nodules. Moreover, stable isotope analysis of pedogenic calcite in the Carlton Heights (~50 km NW of Lootsberg Pass) indicate that pedogenic calcite development in some of these paleosols was influenced by oxidation of organic matter in anoxic environments (i.e., anaerobic microbial decomposition, possibly through sulfate reduction) (Tabor et al., 2007). Thus, poorly drained soil-conditions provided appropriate thermodynamic environments for pedogenic calcite development, and most likely pedogenic gypsum formation (Gastaldo et al., 2020a, 2020c).

The Lebombo Basin paleosols occur approximately 1100 km to the northeast of those in the Main Karoo Basin. Bordy and Prevec (2008) describe a multitude of paleosol morphologies in the Emakwenzini Fm. of the Lebombo Basin. In general, these paleosols are broadly assigned to organic paleosols (coal) and mineral paleosols. The organic paleosols are widely dispersed in the Lebombo Basin, interpreted to be lateral overbank units to low-sinuosity stream systems, reflecting the prevalence of wetland ecosystems in the more proximal areas relative to the basin margin (Bordy and Prevec, 2008). The mineral paleosols include several instances of Protosols and carbonate deposits (Fig. 4) with minimal development of a Bw horizon. Bw horizons are evidenced by: the

development of soil structure; destruction of primary sedimentary structures; and variegated to reddened beds. Plant impressions occur in some of these paleosol profiles. The carbonate beds are interpreted by Bordy and Prevec (2008) to possibly be replacement after a siderite precursor based on the variegated red coloration of the carbonate material, indicating a low oxygen condition poorly-drained environment. If true, then the occurrence of pedogenic siderite in Changhsingian strata in this basin establishes a gradient of redox products Fe²⁺-H₂S--CH₄ by the observed sulfate reduction in the Changhsingian strata of Wapadsberg Pass area of the Karoo Basin (Gastaldo et al., 2020a, 2020b, 2020c), and the interpretation of methanogenesis in the Carlton Heights area of the Karoo Basin (Tabor et al., 2007). If such a redox gradient existed in these paleo-soil systems, then this would provide a new context for interpreting changes to the Late Permian paleoatmospheric composition. For example, Huey and Ward (2005) postulate that lower atmospheric O2 concentrations would have exerted an anoxic control on terrestrial organisms during the EPE. However, such an atmospheric oxygen trend has yet to be demonstrated in biogeochemical models (Lenton et al., 2018), nor has there been confirmation of terrestrial anoxia in paleo terrestrial environments during either the marinedefined EPE or the terrestrial expression of this biotic crisis. Thus, while the Daptocephalus-Lystrosaurus Assemblage Zone predates the marine-defined EPE, a study of redox processes in Late Permian strata terrestrial strata would be instructive in better refining the paleoclimatic and paleoenvironmental change during this time interval.

3.1.4. Transantarctic Basin

The Transantarctic basin preserves both mineral and organic paleosols during the Lopingian. Protosols are the principal mineral paleosol type, and coal is the organic end-member of the paleosol types (Retallack and Krull, 1999; Krull and Retallack, 2000; Sheldon, 2006; Sheldon et al., 2014; Gulbranson et al., 2012, 2020). Protosols of the Transantarctic basins are varied in their composition, and paleolandscape position, such that it is appropriate to consider overbank Protosols and in-channel Protosols as separate environments on these paleolandscapes (Figs. 3C-F, 4, Krull and Retallack, 2000; Gulbranson et al., 2020). Overbank Protosols are the most well-studied and abundant variety and include (Krull and Retallack, 2000; Gulbranson et al., 2012; Sheldon et al., 2014): mottled Protosols; siltstone with low chroma/low value colors of blue-green hue; sandstone with root traces (Fig. 3C&D); shale with carbonaceous root traces; and the Protosol near the lithostratigraphic Permian-Triassic contact (Collinson et al., 1994; Retallack and Krull, 1999). Many of these profiles represent compound or composite soils, indicating changes in landscape aggradation and degradation during the timeframe of pedogenesis (Gastaldo and Demko, 2011). Retallack and Krull (1999) describe paleosols at the Allan Hills locality for Histosols and the sandstone-rich Protosol variant that are clearly compound paleosols. In contrast the shale with carbonaceous root traces is described as a composite paleosol profile. These two intervals are separated by ~10 m of strata indicating the vertical-scale over which changes from aggradational systems to degradational systems took place in the upper Weller Coal Measures. A similar pattern occurs in aggradational depositional settings with laterally continuous overly thick paleosol development. In contrast, degradational depositional environments host compound and laterally-restricted paleosols at the contact between the Weller Coal Measures and Feather Conglomerate (Fig. 3G). Solitary paleosol profiles are described from Graphite Peak as three Protosol variants, distinguished by the type of redoximorphy and soil texture, interpreted to represent a depositional setting in distal area from nearby sediment accumulation areas or active fluvial systems. Several of these Protosols host fossil forests: the siltstone and shale Protosol variants (Graphite Peak; Wahl Glacier; Collinson Ridge); and the sandstone Protosols (Mt. Achernar; McIntyre Promontory; Lamping Peak) (Collinson et al., 2006; Gulbranson et al., 2012; Miller et al., 2016). Significant changes in forest density and leaf habit of the glossopterids (i.e., evergreen glossopterids versus deciduous glossopterids)

correlate with the location of a Protosol environment relative to highly-disturbed riparian environments to emergent landforms proximal to shallow lake basins on the floodplain (Gulbranson et al., 2014).

In-channel Protosols are solitary soil profiles, sand-textured, and are recognized principally because they host in situ fossil forests (Collinson et al., 2006; Gulbranson et al., 2020). As solitary profiles, these paleosols represent a single time frame of pedogenesis balanced against a steady or uniform state of deposition and erosion. In the field, these profiles are recognized as macroform tops in low-sinuosity fluvial environments (Fig. 3C&D, Gulbranson et al., 2020). Dendrochronology of transported fossil wood adjacent to the macroform elements and of in situ fossil wood rooted into the Protosol indicate that fluvial transport of wood was important in generating these emergent landscapes, which remained as forested landscapes on timescales of \sim 100 years. To date, solitary inchannel Protosols are recognized in two localities: Collinson Ridge in the Shackleton Glacier area, hosting an impressive fossil forest of at least 28 in situ trees (Fig. 3D, Collinson et al., 2006); and from the Allan Hills in the upper Weller Coal Measures (Fig. 3C, Gulbranson et al., 2020).

Histosols are abundant throughout the Transantarctic basins. Retallack and Krull (1999) distinguish two types of Histosols on the basis of organic matter decomposition as is done for modern Histosols. Histosols are observed as in situ paleosol layers in overbank facies and as intraformational clasts in lateral and vertically associated sandstones. Like the Lebombo (Bordy and Prevec, 2008) and Sydney basins (Retallack, 1999a), the common occurrence of Histosols in Lopingian strata indicates that widespread peatlands existed on the flood plain adjacent to fluvial systems and shallow lake basins. However, the genesis of these peatlands likely occurred during hiatuses in sediment supply based on detailed fluvial facies analysis (Fielding and Alexander, 2001). Alternatively, a change in local water table elevation through expansion of 2:1 phyllosilicate minerals may also contribute to peat accumulation (Gastaldo, 2010).

In general, Lopingian paleosols in Antarctica represent hydromorphic soil drainage conditions irrespective of being a mineral soil or an organic soil. The wide-spread nature of hydromorphic soils on the paleolandscape gives rise to two main lines of inquiry: 1) what were the factors that could have contributed to such relatively uniform drainage conditions despite variations in soil texture and organic carbon content?; and 2) what effect did this drainage condition have on weathering, soil-formed mineral production, base status, and/or the susceptibility of these ecosystems to ecologic stress (Grime, 1977)? Addressing question 1 requires knowledge of the rainfall inputs, the magnitude and timing of evapotranspiration, and the capacity for drainage systems in the region to organize into a confined flow state (Van der Meij et al., 2018). The Transantarctic basins during the Lopingian likely received lower amounts of annual precipitation (<1000 mm a⁻¹) based on paleosol major element chemistry (Sheldon, 2006; Sheldon et al., 2014), and even less during the early Middle Triassic (~250 mm a⁻¹, Fielding et al., 2019). However, the timing of this precipitation (Fielding et al., 2019) suggests a significant portion fell as snow during the prolonged austral winter. The transition to the austral spring would create a surge of meltwater, unlikely to be fully confined. Furthermore, the austral summer at polar latitudes resulted in months with rainfall greater than evapotranspiration (Fielding et al., 2019). Thus, while the initial spring meltwater surge would have waned, there would still be ample water available under cool/cold summer temperature conditions. When addressing question 2, it is observed that most, but not all, glossopterid forests have been found rooted into mineral Protosols (Fig. 3C-F, Gulbranson et al., 2012, 2014, 2020; Miller et al., 2016). Occurrences of glossopterid forests on peat are evidenced by: in situ stumps found at Collinson Ridge in permineralized peat (Collinson et al., 2006); medium to coarse Vertebraria haloes and permineralizations (specifically Skaar Ridge for very coarse permineralized roots) in numerous Histosols throughout the Transantarctic basins; and facilitative behavior of glossopterids on fallen trees in a permineralized peat deposit at Skaar Ridge (Decombeix et al., 2021). The disparity of fossil forest preservation on

Protosols versus Histosols can be attributed to the following key factors: 1) differential taphonomic preservation of woody tissue in peat versus mineral soil material; and 2) distinct soil conditions (pH, base saturation, etc.) that differed between Protosols and Histosols favoring one form of glossopterid ecosystem development over, perhaps a different one; and 3) the timing of silica-rich waters that promoted silicification of these plant tissues.

3.1.5. Sydney Basin

Paleosols of the Newcastle Coal Measures are divided into two basic types: a Protosol and a Histosol (Retallack, 1999a, 1999b). The Protosols display root haloes, a fining upward texture, and are roughly 50 cm thick (Fig. 4). The fining upward texture is consistent with being a sedimentary artefact rather than a pedogenic feature due to lacking evidence of downward illuviation of material (e.g., clay films/skins/grain bridges). The Protosols and Histosols are in direct vertical association in some measured sections of Retallack (1999a), however, the Protosols also occur within the siliciclastic strata of fluvial and floodplain facies. This indicates two general types of landscape relationships: 1) a change in the landform from mineral soil development to organic soil development (e. g., inundation of water, lower temperatures, low dissolved oxygen content of water); and 2) an alluvial landscape relationship with fluvial and lacustrine systems. The fluvial-flood plain relationship of Protosols is of the alluvial type, where documenting coeval and vertical fluvial facies associations becomes important in distinguishing the relative balance of sedimentation rate and rate of pedogenesis on soil formation.

The Newcastle Coal Measures have been interpreted in a sequence stratigraphic context (Herbert, 1997), with the sandstone lithofacies displaying conspicuously thick macroforms with steeply inclined contacts. These features are interpreted as resulting from homopycnal flow into coastal plain lakes or as crevasse splay deltas. Moreover, the repeated occurrence of base-level fall of 4th order sequences would presumably lead to the development of basin-wide well-developed paleosols at the sequence boundaries (Kraus, 1999). This is an interpretation of 1) very little diversity in paleosol types; and 2) the lack of morphologic development of the mineral paleosols. These sandstones contain an abundance of in situ fossil wood, and numerous paleocurrent orientations and attitude shifts on cross-bedding, indicating their development on emergent landforms in a fluvial setting under variable seasonal discharge and sediment supply (Fielding and Alexander, 2001). Therefore, the alluvial-associated Protosols of the Sydney Basin formed on flood plain settings of low-sinuosity fluvial systems under variable discharge and sediment supply. These conditions likely influenced the development of Protosols as solitary pedons rather than the development of cumulative, composite, or compound profiles.

The basal portion of the Histosols display inclined segmented heterolithic strata. These features have been interpreted as stone rolls, evidence of an active layer in permafrost leading to the disruption of these units (Retallack, 1999a, 1999b). Moreover, the overall wetland type has been interpreted to be specific to extant string bogs, despite the fact that string bogs are not solely endemic to regions with gelic temperature regimes (Heinselman, 1965; Grittinger, 1970). The prevalence of gelic soil temperature conditions in the Sydney Basin is supported by the persistence of the P4 glacial episode into the lowermost Wuchiapingian strata of the Sydney Basin (Metcalfe et al., 2015; Fielding et al., 2019). However, recent climate modeling for the Changhsingian of the Sydney Basin (Fielding et al., 2019) indicates a mean annual soil temperature between 1.5 °C-2 °C, with a mean difference between winter and summer soil temperatures >5 $^{\circ}\text{C}$. The data indicate that this is a cryic temperature regime and thus too warm for permafrost in the top 200 cm of an uncompacted soil. Moreover, paleosols that may have had permafrost are also unlikely to develop a suite of geochemical indicators of paleoclimate as the chemical and mineralogic composition of those soils would not have developed in response to climate/biotic conditions (Gallagher et al., 2019). Thus, permafrost-affected soils were a possibility in this region, only if it is established that gelic materials exist in

these profiles in uncompacted depths <200 cm due to the absence of a gelic temperature regime (Almeida et al., 2014). A gelic temperature regime satisfies the climatic definition of permafrost, thus in the absence of that temperature regime, attention is focused on the depth of an active layer (if present) relative to the primary vegetation type (e.g., moss versus lichen) occupying the soil.

3.2. Sedimentary systems

3.2.1. Sediment transport directions and sources

Sediment transport directions, derived from paleocurrents, are compiled here for each basin to document the alluvial and/or eolian transport directions relative to areas that may have acted as prominent sediment source areas (Fig. 5A). The significance of documenting paleocurrents for sediment transport with regards to paleosol analysis is that 100% of the paleosols compiled herein formed in an alluvial/colluvial setting, meaning that the parent material of these soils was sediment. Thus, sediment transport directions and sediment source areas represent controls on the parent material soil-forming factor (Kraus, 1999; Gastaldo et al., 2014).

The Paganzo Basin and Paraná Basin contain fluvial, and eolian and fluvial paleocurrent data, respectively, with the exception of the Pirambóia Fm. (Zhang et al., 1998; Alessandretti et al., 2016). The Talampaya Fm. of the Paganzo Basin displays E-SE paleocurrents for sheet flood deposits entering a playa lake system, indicating likely local paleoflow in the variable topography of the ancestral Famatina System (Zhang et al., 1998). This is underscored by the onlapping of the Talampaya Fm. with the Nuñorco Granite basement rock and presence of numerous granitic clasts in sheet flood sediments interbedded with the playa lake facies (Gulbranson et al., 2015b). Composition of the Talampaya Fm. reflects a combination of locally-derived material, reworked Lower Permian strata, and Choiyoi volcaniclastic deposits (Gulbranson et al., 2015b; Spalletti and Limarino, 2017). Alluvial and eolian strata of the upper Morro Pelado Mbr. (Rio do Rasto Fm.) of the Paraná Basin indicate N-NW alluvial sediment transport directions, however, eolian deposition displays W-NW paleowind directions (Fig. 5A, Alessandretti et al., 2016). The sediment source areas for the Rio do Rasto Fm. are thought to be the Patagonian volcanic arc system based on U-Pb ages on detrital zircons and EHf results of zircons (Alessandretti et al., 2016; Spalletti and Limarino, 2017). The Pirambóia Fm. represents an additional probable source and storage region of eolian sediment during the Lopingian, however, paleocurrent analysis is lacking from this unit. The available eolian paleocurrents are consistent with Early Permian zonal wind patterns during the austral summer season (Fig. 5B), in which the austral winter zonal wind patterns are $\sim 60^{\circ}$ offset from the summer wind patterns (Horton et al., 2012). This disparity in zonal wind direction alludes to a seasonality in sediment transport in the Paraná Basin. In regards to large-scale teleconnections of eolian dust transport, these paleocurrents further indicate isolation of the available sediment for eolian transport to the Paraná Basin, as zonal wind directions during the austral summer would direct sediment transport to the northwest, away from the Karoo Basin (Fig. 5B).

The Karoo and Lebombo basins paleocurrent results indicate radial drainage extending away from topographically higher basin margins (Smith, 1990; Gastaldo et al., 2014; Bordy and Prevec, 2008; Gastaldo et al., 2021). These paleocurrent data are based on fluvial facies and indicate NE to NW to SE-S paleocurrent directions as one moves from west of 24°E, east of 24°E and to the north in the Lebombo Basin, respectively. Gastaldo et al. (2014) interpreted changes in trace element composition of Changhsingian paleosols of the Karoo Basin (Coney et al., 2007) to reflect a plausible shift in parent material composition on the paleo-land surface, reflecting an increased contribution of volcanogenic material to the Main Karoo Basin during the Late Permian. These inferences are supported indirectly by observations of the anomalously high CIA-K values for Late Permian Protosols (Coney et al., 2007), which may be indicative of contrasting parent material compositions rather

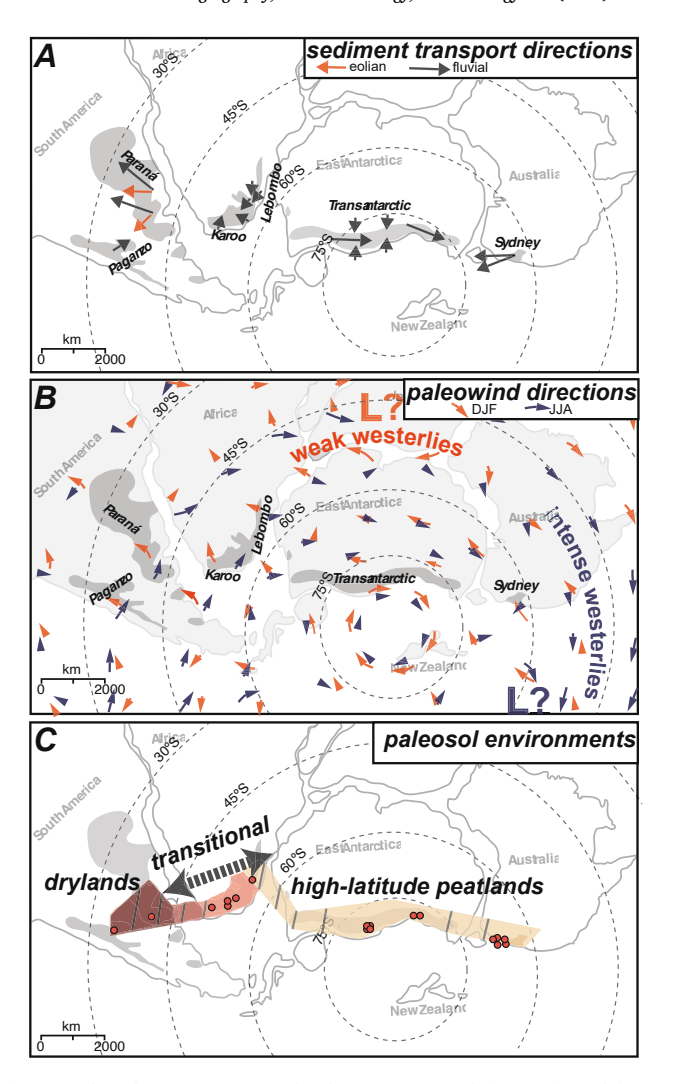


Fig. 5. Paleosol environments and paleoenvironmental factors for soil formation. A) Sediment transport direction based on paleocurrent data. Alluvial transport directions are indicated by the black arrows for each basin, and available eolian paleocurrent data are shown for the Paraná Basin (Pirambóia Fm.), which are consistent with austral summer wind directions over the Paraná Basin (from the Early Permian climate simulation). B) Paleowind trajectories from an Early Permian paleoclimate simulation (Horton et al., 2012). However, the hemispheric climate gradient during the Lopingian was likely very different from these Early Permian simulations, however, the hemispheric organization of wind currents and seasonal variation are important to consider for moistureand sediment-transport. Austral summer (DJF) winds are denoted by orange arrows and text, austral winter (JJA) are denoted by blue arrows and text. Arrow lengths are a suggesting of magnitude. C) Inferred environmental classifications of the study region based on the compilation of work considered herein, dashed where inferred. From west to east: 1) dryland environments of the Paganzo and Paraná basins indicated by the playa lake and 'wet erg', and 'wet erg' fluvial facies associations, respectively (Dias and Scherer, 2008; Gulbranson et al., 2015; Francischini et al., 2018a); 2) a transitional area of the Main Karoo Basin with decreasing seasonal dryness from the area west of 24°E (Smith, 1990, 1995) to east of 24°E (Tabor et al., 2007; Gastaldo and Rolerson, 2008; Gastaldo et al., 2009, 2014, 2015, 2020a; Prevec et al., 2010); 3) highlatitude peatlands with predominantly low-sinuosity fluvial systems characterized by intensely seasonal variation in discharge, and the development of persistent flood plain wetlands with or without organic matter accumulation (Bordy and Prevec, 2008; Fielding and Webb, 1996; Fielding and Alexander, 2001; Fielding et al., 2018, 2019, 2021; Gulbranson et al., 2012, 2014, 2020). (For interpretation of the references to color in this figure legend, the reader is referred to the web version of this article.)

than solely reflecting intense weathering environments. The Lebombo Basin sediment sources are interpreted to reflect cratonic material from an upland area straddling southern Africa and Antarctica during the Lopingian based on the micaceous composition of fluvial sandstones often containing granitic clasts (Veevers and Saeed, 2007; Bordy and Prevec, 2008).

Sediment dispersal patterns of Antarctica and Australia during the Late Permian contrast. Those in Antarctica contain two different drainage patterns. Orthogonal drainage orginiated from the active Gondwanan plate margin and the East Antarctic craton; whereas axial drainage to the southeast along the length of the Transantarctic basins (Collinson et al., 1994). The Transantarctic basins represent two general source area trends for Late Permian sediment. The first is an increasingly volcanic sediment source in the central Transantarctic Mountains as one moves towards the Shackleton Glacier area (Pankhurst, 2002; Collinson et al., 2006; Elliot et al., 2017). Secondly, a predominantly arkosic composition of the Weller Coal Measures (Isbell and Cúneo, 1996). In contrast, fluvial patterns in the Sydney Basin display paleocurrent directions to the S-SW (Fielding et al., 2019) and W-SW (Fielding et al., 2021), and are composed of volcano-lithic sediment compositions influenced by the active margin of Gondwana to the south of the foreland basin (Pankhurst, 2002). Paleocurrents in the Sydney Basin reflect flow from westward cratonic uplands near the margin of the basin, but at the basin-scale the southerly paleocurrent directions suggest flow parallel to the basin axis (Fielding et al., 2020).

3.2.2. Dryland environments

The Paganzo and Paraná basins were occupied by a mosaic of depositional environments. These include: 1) small lacustrine basins (Limarino et al., 2014; Gutiérrez et al., 2018); 2) environments of windblown sediment transport and deposition; and 3) alluvial-fluvial depositional environments. The paleosol record for each basin ranges from cumulative in the Paganzo Basin to solitary and compound in the Paraná Basin. Due to the prevalence of windblown sediment deposition, these paleoenvironments can be classified as dryland systems during the Changhsingian (Fig. 5C). The Paganzo Basin hosts a succession of eolian facies marked by mudstone interbeds and a lack of large-scale crossbedding, interpreted as reflecting a wet-dune type of dryland environment in which windblown dunes were deposited adjacent to ephemeral stream systems (Zhang et al., 1998; facies 6 of Gulbranson et al., 2015b). The Morro Pelado Mbr. of the Rio do Rasto Fm. and the Pirambóia Fm. both preserve eolian deposits in the Paraná Basin, with an abundance of eolian facies in the latter (Lavina et al., 1993; Dias and Scherer, 2008; Francischini et al., 2018a). Like the Paganzo Basin, the Morro Pelado Mbr. and the Pirambóia Fm. do not reflect the classic "dry erg/dune" eolian system. This is due to the limited scale of cross-bedding observed in these strata and common mudstone and fluvial-associated sandstone interbedded throughout the succession. In contrast, the Buena Vista Fm. (Uruguyan sector, Paraná Basin) contains evidence of ephemeral stream deposition under a degradational setting in which compound Protosols developed. The abundant water supply or higher water table elevations of these basins during a relatively arid climate phase must have limited the sediment availability of these systems (Kocurek and Lancaster, 1999). And, combined with the observed paleowind directions, would have further restricted the transport of eolian dust elsewhere on Gondwana.

3.2.3. Alluvial environments and peatlands

Predominantly low-sinuosity fluvial systems are documented across the study region, with the exception of high-sinuosity systems for the Lower Balfour Fm., Karoo Basin (Smith and Botha, 2005). Despite the similarity in fluvial style, and conservative variation of paleosol morphology, sedimentation rates and landscape stability varied appreciably over the study region. This gave rise to successions containing compound or composite paleosol profiles in addition to some other regions containing cumulative or solitary paleosol profiles. Paleosol

profiles in the Karoo Basin, west of 24°E (Fig. 1B, Teekloof Fm.), are preserved as solitary profiles in catena-style relationship (Smith, 1990, 1995). Floodplain paleosols developed adjacent to high-sinuosity fluvial systems with a trend of calcic Protosols in the levee region, Vertisols in the adjacent floodplain areas, and Gypsisols in the distal flood plain areas. However, based on information included in Smith (1990, 1995) from this study area, it is not possible to confidently locate these measured sections to confirm these observations and integrate them into the updated litho/chronostratigraphy of the Karoo Basin. This catena relationships indicates intermittent overbank sedimentation in order to promote the development of morphologically advanced paleosols with highly soluble soil-formed minerals under an arid to semi-arid climate regime. To the east of 24°E in the Karoo Basin (upper Balfour Fm.) paleosols display nuanced trends through time and space. In the lowermost part of the studied strata, compound and composite Vertisols are observed (Gastaldo et al., 2020a) reflecting paleosol development under a seasonal climate on a degradational fluvial landscape. Here, soil moisture conditions reflected highly productive environments (Gastaldo and Rolerson, 2008). At higher stratigraphic positions, east of 24° E, Protosols in overbank environments suggest cumulative profile development in an aggradational setting (Wapadsberg Pass, Fig. 1B, Gastaldo et al., 2014) and successions \sim 15 km away (Lootsberg Pass) and \sim 200 km (Bethulie area; Fig. 1B, Gastaldo et al., 2009) indicate calcic Protosol development under aggradational conditions. These paleosol features form composite profiles, indicative of differential accommodation space along a fluvial gradient. Moreover, isotopic interpretations on carbonate development and occurrence of pedogenic siderite indicate that these paleosols developed in poorly drained conditions, likely with SO₄ or CO₂ reduction (Tabor et al., 2007; Gastaldo et al., 2014). Thus, the drainage area of the Karoo Basin was not uniform in terms of sediment supply and discharge, either along the flow path of these river systems, or laterally from one river system to another. Here, paleosol profiles attest to these subtle differences in fluvial sedimentology through the nature of the profile being solitary, cumulative, composite/compound. These data indicate that the Karoo Basin reflected a poorly-defined climate state, such as those encountered in montane regions, but quite possibly ranging from arid/semi-arid in the western Karoo Basin to sub-humid/ humid in the eastern and northern Karoo Basin (Fig. 5C).

The Lebombo, Sydney, and Transantarctic basins display a similar set of paleosol-alluvial relationships. These regions are here referred to as "peatlands" with the explicit distinction that these were not solely peatforming environments, nor contiguous. Rather, the term "peatland" is intended to refer to the mode of the soil type and paleoenvironment, a wetland that forms peat accumulations. These peat-forming wetlands were coeval to non-peat forming, yet poorly drained mineral soils; and non-wetland depositional systems. Low-sinuosity fluvial regimes dominated these regions, and solitary to cumulative paleosols developed on their distal floodplain settings (Bordy and Prevec, 2008; Fielding et al., 2019, 2021; Gulbranson et al., 2020;). In the proximal floodplain setting compound and composite paleosols are recognized (Retallack and Krull, 1999; Krull and Retallack, 2000; Sheldon, 2006; Gulbranson et al., 2012; Sheldon et al., 2014). Intensely seasonal discharge is consistent with the observed sedimentary structures and stratal architecture of these fluvial deposits (Fielding and Webb, 1996; Fielding and Alexander, 2001; Gulbranson et al., 2020; Fielding et al., 2021). The widespread occurrence of Histosols and densely vegetated, yet morphologically immature Protosol profiles (Fig. 3 C&B, Gulbranson et al., 2012) indicate that peat formation and establishment of perennial non-peat forming wetlands was a dominant process in the region (Fig. 5C). For example, paleooxbow lake deposits recognized in the Karoo Basin showcase the high floral diversity of Glossopteris morphotaxa growing in adjacent non-peat forming environments (Prevec et al., 2009). Glossopterids dominated the arborescent plant taxa and tree rings from these plants demonstrate rapid growth of inexpensive wood (Taylor and Ryberg, 2007). These taxa developed shallow root systems potentially adapted to growth in a hydromorphic setting (Decombeix et al., 2009), which is consistent with

the paleosol morphology and fluvial architecture. The proliferate occurrence of *Glossopteris* leaf macrofossils across Gondwana and these inferences of their growth habits may imply a characterization of the group as hosting a rather simplistic monogeneric forest biome. However, evergreen and deciduous glossopterids are known from stable carbon isotope records of tree rings (Gulbranson et al., 2012); and that these differences in leaf habit correlate to distinct ecologic positions on the paleolandscape in Antarctica (Gulbranson et al., 2014); and in the Karoo Basin (Prevec et al., 2009; Gastaldo et al., 2017). Thus, while the shared factors of depositional setting, paleosol morphology, and plant taxa unite each of these basins, it is probable that variation in the productivity and composition of these peatlands varied across the same area. The expansive glossopterid peatlands and forests of the Lopingian are now known to be absent from Lopingian strata ~370,000 years prior to the marine-defined EPE (Fielding et al., 2019; Mays et al., 2019).

3.3. Molecular weathering ratios

Major element concentrations from sedimentary rocks and paleosol are compiled for the: Paraná, Karoo, Sydney, Bowen, and Transantarctic basins in order to assess the general extents of chemical weathering on land during the Lopingian in southwestern Gondwana. Data exist for sedimentary rocks in general (Goldberg and Humayun, 2010; Metcalfe et al., 2015; Oghenekome et al., 2018; Fielding et al., 2019); and for paleosol-specific analyses throughout a succession of strata (Sheldon, 2006; Coney et al., 2007; Retallack et al., 2011; Gastaldo et al., 2014; Sheldon et al., 2014). Where necessary, these major element concentrations are converted from their reported units (e.g., weight percent oxide) to molar units, and the molar amounts of each oxide are used to calculate the chemical index of alteration minus potash (CIA-K, Mavnard, 1992; Sheldon et al., 2002). The data are binned into Wuchiapingian and Changhsingian stages (Fig. 6A). Vignettes of CIA-K trends as a function of stratigraphic position are maintained in order to illustrate unique paleosol geochemical changes during the Changhsingian (Coney et al., 2007; Gastaldo et al., 2014), or in the lead up to the EPE on Gondwana (Fig. 6B-D, Sheldon, 2006; Retallack et al., 2011).

In general, there exists broad latitudinal variation in CIA-K values during the Wuchiapingian and Changhsingian (Fig. 6A). However, the Wuchiapingian latitudinal gradient in CIA-K is very different from the Changhsingian, displaying a prominent increase in CIA-K values approaching the southern polar region from relatively low CIA-K values in the Karoo Basin. The Changhsingian CIA-K record elicits a total reorganization of chemical weathering on land, most notably for the

Karoo Basin, which saw the greatest overall increase in CIA-K values in the study region during this time (Fig. 6A). In contrast, the Sydney Basin and Transantarctic basins reflect a decrease in CIA-K value into the Changhsingian. However, this may reflect a sampling deficit of early Lopingian strata in Antarctica, as the stratigraphic record of CIA-K values there indicated pronounced increases near the Permian-Triassic stratigraphic contact (Fig. 6D, Sheldon, 2006; Sheldon et al., 2014). Moreover, this bias also extends to the Karoo Basin, which reflects a much higher sampling density than adjacent basins. The Paraná Basin sedimentary record (with its caveat) and the Sydney Basin paleosol CIA-K values are invariant at the stage-level. However, the Sydney Basin molecular weathering ratios exhibit a pronounced increase near the Permian-Triassic contact (Fig. 6C, Retallack et al., 2011; Fielding et al., 2019; Frank et al., 2021), despite similar distributions of CIA-K values during Wuchiapingian time. Thus, while significant changes in CIA-K value, and potentially chemical weathering on land, occurred in the Karoo and Transantarctic basins during the Lopingian (Fig. 6B&D, Sheldon, 2006; Gastaldo et al., 2020a, 2020b, 2020c), this pattern was not universal across Gondwana.

The trend of CIA-K values over time and space presents a unique problem to Lopingian soils on Gondwana. Of all the basins in this study region, the Karoo Basin preserves the widest array of paleosol morphologic variation and the highest degree of morphologic development (as a function of fluvial system state). Excluding the dryland depositional basins (Paganzo and Paraná basins), this leaves the Lebombo, Sydney, and Transantarctic basins as displaying three paleosol orders. These are Gleysols, Protosols and Histosols of equivocal morphologic difference within the respective orders. Thus, there is a greater variance in the geochemical development of Protosols on Gondwana, standing in stark contrast to the conservative nature of development of these predominantly hydromorphic paleosols.

We applied the paleohumidity and floral province proxy (Gulbranson et al., 2011) to further evaluate these major element data. Net primary productivity (Fig. 7, see section 3.4.1), mean annual precipitation, and potential evapotranspiration are inferred from CIA-K and CIA values, and paleosol morphology (Fig. 8). However, we rely on paleoclimate simulations for the Late Permian (Kiehl and Shields, 2005; Fielding et al., 2019) and independent estimates of paleotemperature (Gastaldo et al., 2020a) to constrain the ranges of temperatures and rainfall amounts for these anomalously high CIA-K values of the paleopolar regions. The results of these analyses agree well with independent observations/measurements of plant productivity and paleotemperatures. However, we recognize a dearth of parent material to subsoil

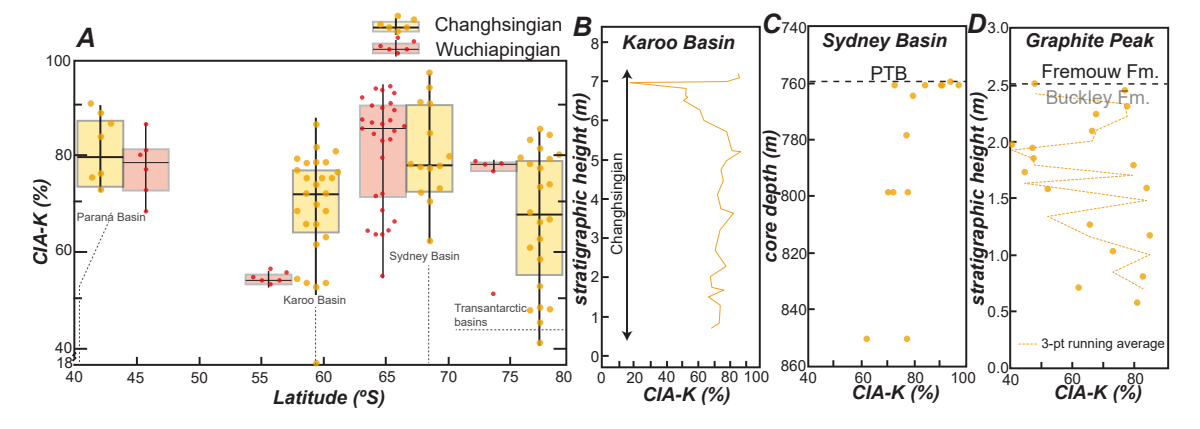


Fig. 6. Molecular chemical weathering proxies for the study region. A) compilation of CIA-K values for the Lopingian over the latitudinal range of the study area. Data are binned for Wuchiapingian strata relative to Changhsingian strata. Wuchiapingian CIA-K values for the Karoo Basin are from Oghenekome et al. (2018); Wuchiapingian CIA-K values for the Sydney Basin are from Retallack et al. (2011); and Wuchiapingian CIA-K values for the Transantarctic basins are from Sheldon et al. (2014). B–D represent stratigraphic vignettes of CIA-K values during the Changhsingian and including the Permian-Triassic boundary (PTB) to illustrate the temporal changes in CIA-K values across the study area during the Changhsingian and the inference of increased chemical weathering across the PTB. B) Karoo Basin Changhsingian CIA-K values (Coney et al., 2007; Gastaldo et al., 2014). C) Sydney Basin Changhsingian CIA-K values (Retallack et al., 2011). D) Transantarctic Basin Changhsingian CIA-K values (Retallack and Krull, 1999; Sheldon, 2006).

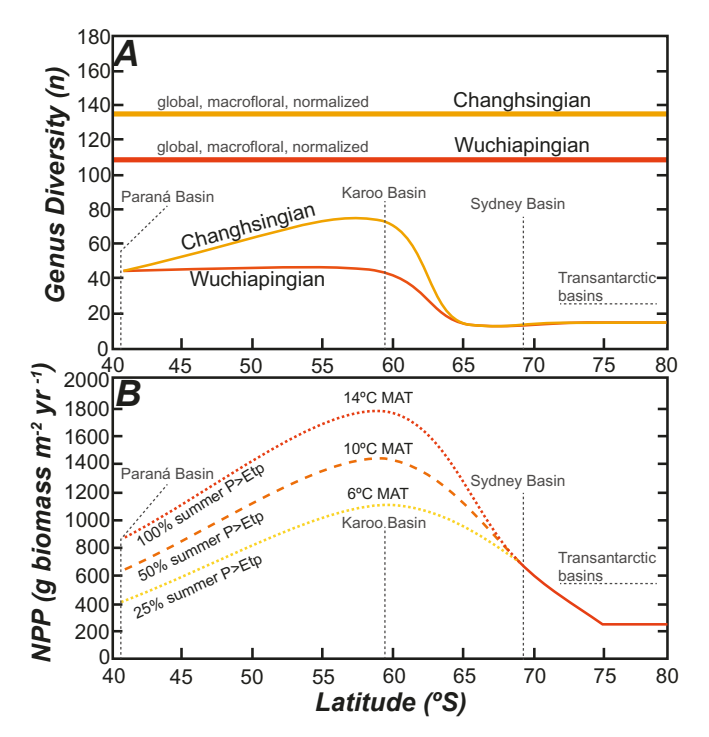


Fig. 7. Floral diversity and estimated net primary production (NPP). A) Generic diversity for macroflora during the Lopingian, comparing global records (the gymnosperm macroflora data from Nowak et al., 2019) and Gondwanan generic diversity (Rees, 2002) over the study region. B) NPP estimated from the equation of Lieth (1975) and checked against estimated of biomass productivity for the Transantarctic basins (Ryberg and Taylor, 2012; Miller et al., 2016). The NPP curve is solid where these estimates are independently checked or based on numerical climate simulation that produces monthly mean temperatures (Fielding et al., 2019). The dashed portion of the NPP curve reflects uncertainty given in paleotemperature estimates from Gastaldo et al. (2020a) of 10 \pm 4 $^{\circ}\text{C}$ for the Karoo Basin, and for the Paraná Basin, which is based on the Late Permian paleoclimate simulation of Kiehl and Shields (2005) modified to reflect a contribution of 100% of the summer temperatures for plant growth, 50% of summer temperatures for plant growth, and 25% of summer temperatures for plant growth. The assumption is that P > Etp for the specified duration of summer temperature conditions. Given the arid paleoenvironmental interpretations of the Paraná Basin, a 25% duration seems more likely. Paleorainfall estimates, ~ 1100 mm $a^{-1} \pm 180$, from Gastaldo et al. (2020a) and inferred seasonality of rainfall were used to determine the number of months when P > Etp for Karoo Basin NPP estimates.

comparisons of major element and mineral compositions in this data set. Such comparisons are vital towards selecting paleosols that demonstrate a clear geochemical alteration of the parent material into soil-formed material, provisionally set at those paleosols that have a CIA-K value of the subsoil 5% or more than the parent material (Sheldon et al., 2002; Gulbranson et al., 2011). Comparisons of paleosols along lateral transects, where applicable, and appropriate sampling density are highly recommended for future work in paleoclimate reconstructions (Dzombak et al., 2021).

3.4. Paleobiology

3.4.1. Paleoflora

Upper Permian Lopingian floras on Gondwana were dominated by a sole arborescent gymnospermous taxa, the glossopterids, and numerous forms of understory vegetation in the form of ferns, lycopsids, sphenopsids, and bryophytes (Cúneo et al., 1993; Pigg and Taylor, 1993; Pigg and McLoughlin, 1997; Iannuzzi, 2010; Prevec et al., 2010; McLoughlin, 2011; Schwendemann et al., 2010; Ryberg et al., 2012). The floral diversity of Gondwanan ecosystems was generally lower than in other

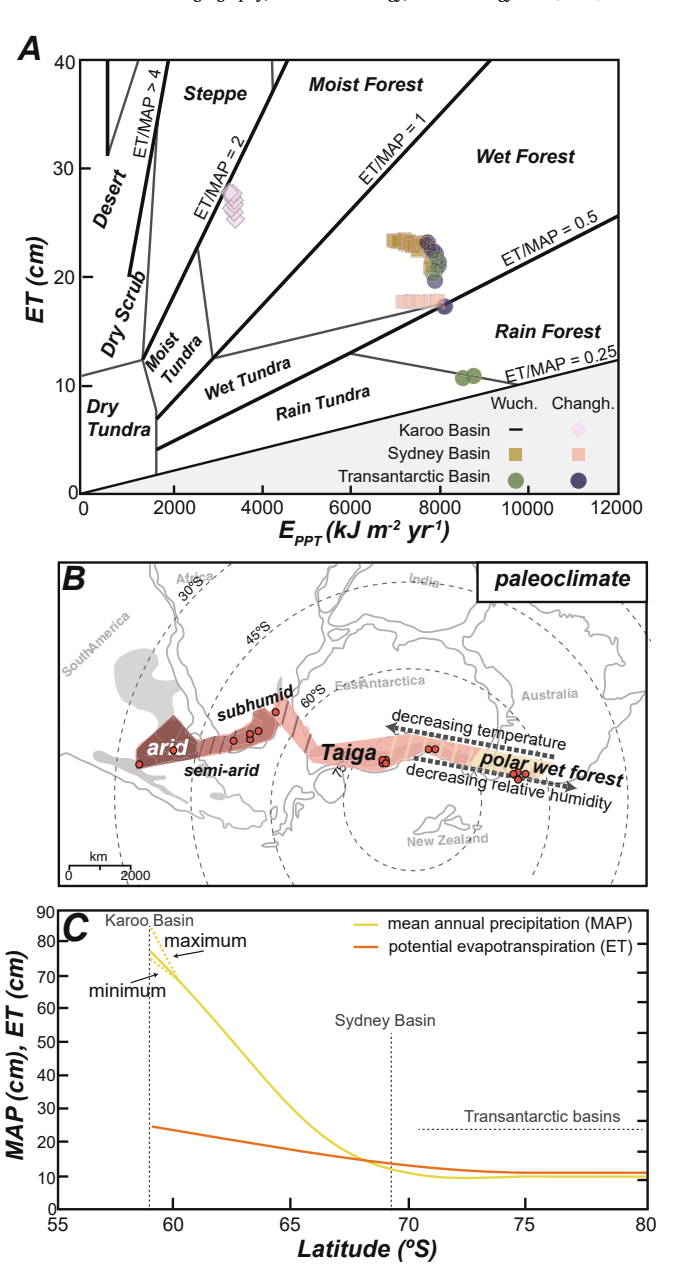


Fig. 8. Paleosol-based Changhsingian paleoclimate interpretations for regions with paleosol-derived CIA-K and CIA values. A) paleohumidity and floral province (after Gulbranson et al., 2011) for the Karoo, Transantarctic, and Sydney basins. B) Paleoclimates superimposed on the study area, dashed where inferred. Taiga is interpreted to reflect the broad afforestation of the polar regions, as modern climate classifications lack a specific category for this unique biome. The distinction between the Sydney and Transantarctic basins, despite plotting in the same field in Fig. 8A, is noted as a function of relative humidity and temperature differences between the two basins. C) Mean annual precipitation (MAP) and potential evapotranspiration (ET) for the Karoo, Sydney, and Transantarctic basins. A range of MAP values is shown for the mean, maximum, and minimum CIA-K values in the Karoo Basin. The range of ET values for the Karoo Basin is too limited to display.

floral realms (Angara, Euramerica, Cathaysia) throughout the Permian (Rees, 2002; Fig. 7A). Generic diversity of flora during the Lopingian, however, displays a dramatic increase in the Karoo Basin from the Wuchiapingian to the Changhsingian (Rees, 2002), and nadir in the Transantarctic basins. Global compilations of generic macrofloral diversity exhibit the opposite trend, a slight decline from the Wuchiapingian to the Changhsingian (Nowak et al., 2019; Fig. 7A), which has been used to suggest provincial responses to the factors that controlled

floral diversity during this time. Moreover, the regional diversity trends across Gondwana allude to pronounced differences in the organismal state-factor for soil formation, where plants are envisioned as providing crucial subsidies of reagents to the soil system that influence water holding capacity and biochemical reactions within the soil system. For example, phosphorous abundance in modern soils correlates well with soil order in the USDA system as well as biome (Dzombak and Sheldon, 2020).

The productivity of these ecosystems in response to Late Permian environmental and climatic change is estimated from the relationship of net primary production (NPP) to monthly temperature (Lieth, 1975; Gulbranson et al., 2011), in order to evaluate the impact on plant diversity gradients to soil systems on Gondwana. The estimated NPP values are independently assessed to the per capita biomass production rate from Miller et al. (2016) and whole-plant mass of Ryberg and Taylor (2012). An estimated NPP of 251 g biomass m⁻² yr⁻¹ for Lopingian climates of Antarctica (Gulbranson et al., 2020) is equivalent to 628 g biomass tree⁻¹ yr⁻¹ for a tree density of 0.4 trees ha⁻¹ (based on inchannel fossil forests from the Weller Coal Measures), which is within the range estimated by Miller et al. (2016). These per capita biomass accumulation rates would achieve the estimated whole-plant biomass from Ryberg and Taylor (2012) in ~109 years, which is well within the lifespan of most glossopterid stems in Antarctica. Thus, estimated NPP for the Lopingian of Antarctica is in agreement with two independent estimates of biomass productivity based on fossil tree ring analysis. These NPP calculations are extended across the study region for the paleoclimate results of Fielding et al. (2019) for the Sydney Basin, for Gastaldo et al. (2020a) for the Karoo Basin, and a range of possible seasonal temperatures for the Paraná Basin based on the climate simulation of Kiehl and Shields (2005). The resulting NPP curve (Fig. 7B) indicates a parabolic trend in NPP as a function of paleolatitude, similar to the genus diversity curve for the region.

The results of the NPP analysis and compilation of generic macrofloral diversity reveal that the Karoo Basin experienced the largest change in macrofloral diversity in the Lopingian, and likely maintained the largest potential NPP in the region. These two factors are likely to explain: 1) the greater extent of paleosol morphologic development; and 2) the drastic increase in paleosol CIA-K values during the Lopingian. Moreover, despite an invariant diversity record through time, the NPP rates for the Sydney and Transantarctic basins reflect the potential for significant organismal effects on soil systems, given the abbreviated growing season at these high paleolatitudes. Thus, inferences of enhanced chemical weathering on land during the EPE in Antarctica (Sheldon, 2006) are highly likely, given the diversity of forest structure and composition across the Transantarctic basins lending greater chemical weathering potential to higher density forest stands than lower density stands.

3.4.2. Paleofauna, vertebrates

The vertebrate record across Gondwana reflects a diverse faunal assemblage, with distinct regional composition. A relatively diverse assemblage of temnospondyls is known from the Buena Vista Fm. (Uruguyan Paraná Basin) (Piñeiro et al., 2012; Ernesto et al., 2020). However, what is most notable about the southern Paraná Basin vertebrate assemblage is the absence of the therapsids, which are well represented in the adjacent Karoo Basin (Smith and Botha, 2005) and evidence of dicynodonts from the Brazilian sector of the Paraná Basin (Francischini et al., 2018b). Other vertebrates preserved in the Paraná Basin include lungfish as evidenced by calcified aestivation chambers in the Serrinha Member of the Rio do Rasto Fm. (Francischini et al., 2018a). The Karoo Basin hosts an exceptional faunal record from the Late Permian and into the Early and Middle Triassic (Smith and Botha, 2005; Botha and Smith, 2007). For the Lopingian, the Daptocephalus and Lystrosaurus declivis Assemblage Zones document Lopingian terrestrial vertebrates. However, a severe lack of reliable location data for accessioned specimens, for stratigraphic position and correlation, and

problematic assignment of biozones to available geochronology hamper refined study against paleoenvironmental and paleoclimate change during the Lopingian (Gastaldo et al., 2019). The potential lifestyle of these organisms are interpreted as herbivorous with a fossorial habit (Smith and Botha, 2005; Bordy et al., 2011), and potentially amphibious (King and Cluver, 1991). High-resolution analysis of Lystrosaurus tusks from Antarctica reveal evidence for seasonal dormancy or hibernation of polar-latitude dicynodonts (Whitney and Sidor, 2020). The reported transition of the Daptocephalus AZ to the L. declivis AZ (Retallack et al., 2003; Botha and Smith, 2007; (Viglietti, 2020)) is now known to have occurred in the Changhsingian, although Gastaldo et al. (2021) demonstrate that these Assemblage Zones are not unique in space and time. This faunal transition, if it exists, is envisioned by Viglietti et al. (2018) as driven by an increase in soil drainage conditions in the Balfour Fm., which may be a local phenomena given the range of soil morphologies and inferred drainage across the Karoo Basin during the Lopingian.

3.4.3. Paleofauna, ichnofossils

At the global-scale, Late Permian trace fossil associations display a change in behavior and life strategies relative to the Early and Middle Permian, resulting in a decrease in genus ichnodiversity. The decrease in ichnodiversity is accompanied by a reduction in architectural design, ecospace occupation, and ecosystem engineering (Minter et al., 2016). Within the Late Permian, however, a latitudinal gradient in plant-insect interactions is evident from leaf macrofossils that is interpreted to reflect greater diversity of plant-insect behavior in the paleotropical latitudes and increasingly less diverse relationship towards the paleo high-latitudes (Liu et al., 2021). Ichnofossils reported below are organized as follows: playa lake ichnofossils/ichnofacies; vertebrate trace fossils; insect feeding traces and invertebrate traces in terrestrial non-playa environments.

Playa lake deposits of the Talampaya Fm., Paganzo Basin, hosts a diverse array of ichnofauna: *Cruziana problematica, Diplocraterion* (isp.), *Merostomichnites aicuñai, Mirandaichnium famatinense, Monomorphichnus lineatus, Palaeophycus tubularis, Umfolozia sinuosa*, and *Umfolozia longula* (Zhang et al., 1998). These include a wide array of aquatic behavior in the playa lake system in the upper portion of the Talampaya Fm. Pond deposits from the Newcastle Coal Measures, Sydney Basin preserve conchostracans, *Permosyne* beetles, and insect larva (Beattie, 2007).

The Pirambóia Fm. of the Paraná Basin preserves evidence of tetrapod ichnofossils *Chelichnus* and *Dicynodontipus*, indicating that that dicynodont activity continued in the Paraná Basin during the wet-erg phase of the basin evolution (Francischini et al., 2018b). In contrast, the vertebrate fossil record to the south in the Paraná Basin provides no evidence for the presence of dicynodonts (Ernesto et al., 2020). The Sydney Basin documents a decrease in ichnofabric diversity from the last marine strata related to the P4 glaciation to the fully terrestrial strata of the remainder of the Lopingian (Fielding et al., 2019), but includes large trace fossils of *Reniformichnus australis* (McLoughlin et al., 2020), associated with vertebrate burrows immediately overlying the EPE horizon.

The Karoo Basin hosts a range of ichnofacies in the form of trace fossils and insect-plant interactions (Prevec et al., 2010), including invertebrate trace fossils such as *Katbergia* (Gastaldo and Rolerson, 2008). Insect-body fossils are widely reported from the Normandien Fm. (Van Dijk, 1998; Van Dijk and Geertsema, 1999) and there is a single report from the Lebombo Basin (Aristov et al., 2009). The Transantarctic basins display a predominantly alluvial ichnofacies. The Feather Conglomerate has evidence of *Skolithos* (Fitzgerald and Barret, 1986); whereas the Buckley Fm. contains ichnotaxa such as *Cruziana*, interpreted to reflect occupation of fluvial macroforms during seasonal reduction in discharge (Miller and Collinson, 1994). *Diplichinites* is also observed in the Buckley Fm. in fine-grained parallel bedded units, as a potential flood plain ichnotaxa (Briggs et al., 2010). Ichnofossils of plant-insect interactions are recorded from lagerstätte in the Sydney Basin, which preserve a range of coeval depositional environments

(Beattie, 2007). Swampland and riparian paleoenvironments include phloem-feeding Hemiptera and pollinivorous and detritivorous Mecoptera (Beattie, 2007). Whereas, bark dwelling arthropods in the Sydney Basin are recognized as Protelytroptera, Psocoptera, and Coleoptera (Beattie, 2007).

4. Discussion

4.1. Latitudinal trends in soil-formation during the Lopingian

Five paleosol orders are observed across the study region: 1) Protosols, 2) Vertisols, 3) Gleysols, 4) Calcisols, and 5) Histosols. Gypsisols may occur in the Karoo Basin (Smith, 1990, 1995), but the location reported for these Gypsisols is insufficiently precise to verify their existence, nor have Gypsisols been observed elsewhere in the Karoo Basin. These paleosols are not uniformly distributed across Gondwana, although current data indicate that the Karoo Basin preserves the greatest diversity of soil-forming environments during the Lopingian (Fig. 4). Moreover, the diversity of paleosol morphologies decreases towards the upper Changhsingian strata (Fig. 4). These paleosol distribution patterns represent broad-scale organization of three distinct soilforming environments: drylands, a transitional region, and a broad highlatitude peatland (Fig. 5C), with further subdivisions in each. Dryland environments contain evidence of increasing aridity through time: transitioning from fluvial deposition to increasingly eolian deposition in the Paganzo Basin (Zhang et al., 1998; Gulbranson et al., 2015b); in the Paraná Basin a change from Vertisols to Protosols during the Lopingian (Francischini et al., 2018a; Ernesto et al., 2020); and the Karoo Basin west of 24°E displays evidence of soil-formed gypsum and calcite in a high-sinuosity fluvial/alluvial setting (Smith, 1990, 1995). The transitional region displays prominent changes in paleosol drainage conditions and sedimentation rate (Gastaldo et al., 2009, 2014, 2020a, 2020c), as well as distinct redox states of the paleo soil-forming environment (Tabor et al., 2007). The peatlands contain evidence of frigid/ cryic wetland conditions in the Sydney Basin (Retallack, 1999a, 1999b), persisting throughout the Lopingian (Fielding et al., 2019); similar temperature regimes likely existed for the Lopingian equivalents in the Transantarctic basins (Fig. 8B).

Chemical weathering in paleosols and sediments during the Lopingian display prominent latitudinal variation (Figs. 6A, 8A), with the Karoo Basin displaying a significant increase in chemical weathering during the Changhsingian relative to the Wuchiapingian. Similar latitudinaly trends are seen in modern soil systems, with higher latitude soils exhibiting a diverse range of CIA-K value based on parent material (Dzombak and Sheldon, 2020). The Karoo Basin paleosols, however, reflect the highest sample density for major element and stable isotopic data of Lopingian paleosols on Gondwana, reflecting a sampling bias. Furthermore, the high degree of chemical weathering inferred from paleosol CIA-K values for the paleo-high latitudes (Sydney and Transantarctic basins) is a surprising outcome of this review, given the conservative nature of paleosol morphology and similar plant taxa in these regions (Fig. 7A). These latitudinal patterns indicate a radically different hemispheric gradient in moisture and heat transport during the Lopingian (Fig. 8C), as compared to the modern, in order to generate the enhanced chemical weathering on land as is observed at the paleo-high latitudes (Sheldon, 2006). Moreover, the marked increase in chemical weathering in the Karoo Basin during the Changhsingian and the time equivalent increase in macrofloral generic diversity (Fig. 7A) portends a prominent shift in terrestrial ecology during this time. Such a diversity change could have had a direct impact on the soil weathering environment due to enhanced production of organic acids from organic matter decomposition and as an energy subsidy to the soil environment.

4.1.1. Shifting fluvial regimes

A transition from high-sinuosity fluvial systems to low-sinuosity fluvial systems has been invoked as a prominent aspect of the EPE on

Gondwana, attributed to the absence of rooted riparian environments as a consequence of the EPE on land (Ward et al., 2000; Smith and Botha, 2005; Retallack et al., 2006; Sheldon et al., 2014). However, many of the basins considered herein contained prominent low-sinuosity fluvial systems throughout the Lopingian and into the Induan, or display the opposite trend of fluvial facies through time. The Lopingian Emakwezini Fm. alluvial environment is interpreted as a low-sinuosity stream system with associated floodplain lakes and wetlands (Bordy and Prevec, 2008). A similar situation is reported by Gastaldo et al. (2021) for the Main Karoo Basin. The Buena Vista Fm. contains evidence of low-sinuosity ephemeral fluvial deposition (Ernesto et al., 2020). The lowermost Weller Coal Measures is interpreted as hosting low-sinuosity fluvial systems near the basin margin and high-sinuosity fluvial systems draining along basin-axis (regarding the strike of this longitudinal basin) (Isbell and Cúneo, 1996). The uppermost portion of the Weller Coal Measures and the overlying Feather Conglomerate are interpreted as a low-sinuosity stream system with flood plain wetlands (Fig. 3G, Isbell and Cúneo, 1996; Liberato et al., 2017), and in-channel glossopterid forests (Gulbranson et al., 2020), shifting to high-sinuosity systems with forested riparian environments in the overlying Lashly A Fm. of early Middle Triassic age (Gulbranson et al., 2020). The Upper Buckley and Lower Fremouw fms. (in the Shackleton Glacier area, inclusive of Graphite Peak) represent low-sinuosity stream systems during the Changhsingian (Collinson et al., 2006), with prominent in-channel forests and flood plain peatlands and non-peat-forming wetlands (Gulbranson et al., 2012). The Sydney Basin likewise contains widespread examples of in-channel glossopterid forests (Fielding and Alexander, 2001; Fielding et al., 2019) along with flood plain wetland ecosystems within an overall low-sinuosity fluvial environment that remained consistent from the Lopingian through the Early Triassic (Fielding et al., 2019, 2021). Thus, there is unambiguous consistency of river morphology in the lead up to the EPE or across the Permian-Triassic boundary across Gondwana. Changes in fluvial morphology during this time, therefore, are likely related to an ensemble of local climate, tectonic, landscape, and ecologic factors, as opposed to a single global/ hemispheric mechanism.

For example, the propensity of water availability from snowmelt during the early growing season at high-latitudes has been proposed to explain convoluted macroform associations in Lopingian fluvial strata (Fielding and Alexander, 2001; Gulbranson et al., 2020), where similar in-channel macroform and sedimentary structure associations are observed in the Emakwezini Fm. (Bordy and Prevec, 2008); and a similar waterlogged nature of low-sinuosity fluvial deposition is observed in the Lopingian Bainmedart Coal Measures of the Lambert Graben, East Antarctica (Fielding and Webb, 1996). These ancient examples of fluvial environments have been classified based on the variance of discharge (Fielding et al., 2018), further underscoring the importance of sediment supply versus water supply in controlling fluvial facies and architecture. Thus, a change in precipitation regime and winter temperatures (e.g., Fielding et al., 2019, Fig. 8A) could directly have affected the timing and magnitude of discharge and sediment supply without requiring the invocation of an apocalyptic wasteland. Tectonic activity along the active-margin of Gondwana could likewise affect fluvial morphology and grain size trends, through changes in subsidence or emergence of new sediment-source areas (Gastaldo et al., 2014).

4.1.2. Soil drainage and low oxygen conditions

The Karoo Basin preserves a wide range of soil drainage conditions throughout the Lopingian and across the basin (Smith, 1990, 1995; Gastaldo and Rolerson, 2008; Gastaldo et al., 2009, 2014, 2020a). Poorly-drained wetland environments prevailed in the Lebombo Basin (Bordy and Prevec, 2008), in which pedogenic siderite may have accumulated. To the south, near Carlton Heights (Fig. 1B), poorly drained wetlands are inferred from stable isotope geochemistry on pedogenic calcite, suggesting potential CO₂-reduction pathways in these paleoenvironments (Tabor et al., 2007). Approximately 55 km south of

Carlton Heights, at Wapadsberg Pass, pedogenic pyrite is observed ubiquitously in Protosols, also indicative of poor soil drainage, but with different redox chemistry (Gastaldo et al., 2014). The sequential reduction of Fe³⁺ to Fe²⁺, SO_4^{2-} to H_2S , and CO_2 to CH_4 is known as a redox ladder (Dzombak and Sheldon, 2020), which is a concept that ranks redox poise by their energy yield for microbially-mediated reactions. The exhaustion of a preceding redox reagent (e.g., Fe³⁺) would necessitate the use of the next energetic reagent in the absence of dissolved oxygen (e.g., SO_4^{2-}). However, it is important to understand if these redox-sensitive soil-formed minerals formed contemporaneously in the Karoo and Lebombo basins during the Changhsingian, and/or over what time range did these redox-sensitive soil-formed minerals develop. If contemporaneity can be demonstrated, then the observed soil-formed minerals and/or interpreted paleo soil-chemical conditions indicate that a gradient of increasingly anoxic and sequentially Fe-SO₄ starved pore waters existed in the Karoo and Lebombo basins. If this hypothesis withstands subsequent analysis, then this can be used to offer an alternative to the hypothesis that a decline of global tropospheric O₂ contributed to the terrestrial EPE (Retallack et al., 2003; Huey and Ward, 2005). Rather, this hypothesis could more parsimoniously be explained as reflecting regional differences in soil redox conditions and drainage. Moreover, the timing and duration of these redox-sensitive mineral accumulations would be essential for further evaluating the paleoclimate and paleoenvironmental changes Changhsingian.

A notable change in soil redox state is observed in the Transantarctic basins (Sheldon, 2006) through increases in the $\mathrm{Fe}^{2+}/\mathrm{Fe}^{3+}$ ratio and increase in Eu and Ce content in earliest Triassic paleosols as compared to upper Changhsingian paleosols. The mineral berthierine is cited as evidence of prevalent reducing conditions in latest Permian paleosols (Retallack and Krull, 1999; Krull and Retallack, 2000; Retallack et al., 2006); however, the interpretation of berthierine as a soil-formed mineral is problematic as berthierine is demonstrated to be a diagenetic product of kaolinite reduction in Fe- and Mg-rich aqueous environments (Bhattacharyya, 1983). Examples of berthierine in coal are based on siderite-kaolinite reactions that occured in the hypogene environment (Iljima and Matsumoto, 1982), and as a polymorph of Fe-rich chlorite (Xu and Veblen, 1996). Therefore, berthierine is more likely evidence of the diagenetic history of these paleosols, whereas the major and trace element geochemistry (Sheldon, 2006; Sheldon et al., 2014) is more instructive on their redox state.

4.1.3. Soil erosion

Soil erosion, referred to as a crisis, has been invoked for the latest Permian succession in Antarctica and elsewhere as a symptom of deleterious environmental conditions on land during the EPE (Retallack, 2005; Retallack et al., 2006). However, intraformational conglomerates with mudstone (often displaying root haloes) and peat clast compositions occur throughout Late Permian, Early Triassic, and early Middle Triassic strata in Antarctica (Fielding and Webb, 1996; Isbell and Cúneo, 1996; Collinson et al., 2006). These are often coeval with stratigraphic intervals containing abundant fossil wood, in situ forests, or intact peat accumulations (Cúneo et al., 1993, 2003; Gulbranson et al., 2012). Abundant intraclasts of overbank material, including vertebrate remains, occur throughout the Buena Vista Fm. of the Paraná Basin (Ernesto et al., 2020). Moreover, the soil erosion "crisis" interpreted for the Karoo Basin exists as intraformational conglomerate in a single channelized deposit with no lateral correlative units of similar aspect (Gastaldo et al., 2009), and mudclast aggregates are a common component in these lag deposits (Gastaldo et al., 2013). In fact, episodes of erosion and deposition of riparian material including soil and woody debris has been invoked as an important biogeomorphologic control on Late Permian low-sinuosity fluvial environments in Antarctica and Australia (Fielding and Alexander, 2001; Fielding et al., 2018), with dendrochronology demonstrating synchronicity between woody debris deposition and the establishment of forested channel macroforms

(Gulbranson et al., 2020). Thus, the cycling of overbank material into inchannel depositional systems contains more evidence of being a common process, and perhaps transformative for the paleo-landscape. It acted as a mechanism to open-up new regimes for plant growth rather than a symptom of a depauperate landscape devoid of the slope stabilizing capability of perennial root systems.

4.1.4. Aridity

Aridity is inferred as both a regional trend during the Lopingian and EPE, and also as a global climate shift (Retallack et al., 2003, 2006; Smith and Botha, 2005). However, this analysis of paleosols does not support a global aridification event outside the occurrence of dryland paleoenvironments in the Paganzo and Paraná basins (Figs. 5C, 8A&C). The development of dryland environments in these basins could reflect an expansion of the mid-latitude downwelling arm of the southern Hadley Cell during the Lopingian as evidenced by the Coriolis-deflected equatorward paleowind direction from eolianites in the Paraná Basin (Alessandretti et al., 2016). Interpretations of aridification from the Late Permian into the Early Triassic in the Karoo Basin, however, rest primarily upon two factors: 1) the occurrence of pedogenic calcite in Late Permian and Early Triassic paleosols (Retallack et al., 2003); and 2) the occurrence of red beds as compared to variegated to non-red bed strata lower in the stratigraphic succession (Smith and Botha, 2005; Ward et al., 2005). Pedogenic calcite in the Karoo Basin has been demonstrated to reflect carbonate development under both poorly drained soil conditions and variable redox states (Tabor et al., 2007; Gastaldo et al., 2014), however, these conclusions have been challenged by Retallack (2021). Moreover, detrital pedogenic calcite in the uppermost Balfour Fm. has been demonstrated to reflect polygenetic soil development and host geochemical artefacts of both seasonally dry open-system soil conditions and a later stage poorly drained closed system condition, consistent with a trend through time of in situ pedogenic calcite in the Balfour Fm. (Gastaldo et al., 2020c). Color mottling is expressed as lateral variation throughout the Changhsingian, and is not restricted to either the Lystrosaurus-Daptocephalus Assemblage Zone or provisional stratigraphic succession contemporaneous with the EPE (Gastaldo et al., 2014). Moreover, red beds are not de facto evidence of aridity (Sheldon, 2005; Li et al., 2017), where the red color is principally due to the occurrence, or removal, of Fe³⁺ (oxy)hydroxide minerals through different means. The first may be the introduction of eolian dust (Amit et al., 2020), or, secondly, as an outcome of several possible diagenetic conditions that are affected by the porosity and permeability of the host rock (Chan et al., 2000; Chan et al., 2005). The observed change in sedimentary rock color in the Karoo Basin has been shown to reflect: 1) diagenetic conditions; and 2) the influence of variable soil drainage during the Changhsingian that accumulated sufficient Fe²⁺ to promote diagenetic oxidation to hematite (Li et a., 2017; Gastaldo et al., 2021). The Sydney Basin likewise contain evidence of limited changes to fluvial discharge during the Late Permian-Early Triassic (Fielding et al., 2021), and a shift towards possibly higher rainfall amounts into the Early Triassic (Retallack, 1999a, 1999b; Fielding et al., 2019). The Transantarctic basins do not contain evidence of increased aridity through the Lopingian (Fig. 8A). Rather, the paleosol data indicate persistent waterlogging of the land surface (Retallack and Krull, 1999; Krull and Retallack, 2000; Gulbranson et al., 2012, 2020), and enhanced chemical weathering in mineral paleosols under a plausibly warmer climate (Sheldon, 2006).

5. Conclusions

Five paleosol orders are observed to occur across Gondwana during the Lopingian: Protosols, Vertisols, Gleysols, Calcisols, and Histosols. These paleosols are not uniformly distributed across the southern hemisphere or through time during the Lopingian, giving rise to distinct soil-forming regions across Gondwana and through time. Dryland environments were restricted to the western sector of Gondwana,

characterized by: cumulative Protosol profiles, eolianites, and playa lake deposits in the Paganzo Basin; the vertical transition from Vertisols and Calcisols to eolianites, ephemeral stream deposits, and cumulative Protosols in the Paraná Basin; and the production of soil-formed gypsum in the western Karoo Basin. A transitional region is envisioned for the eastern Karoo Basin with drainage-dependent and sediment supply-dependent association of Vertisols and Protosols, displaying evidence for increasing humidity through time. A broad region of Histosol development, high-latitude peatlands, and highly seasonal fluvial discharge and Protosol development is observed in the Lebombo, Transantarctic, and Sydney basins, with possibly frigid/cryic peatlands in the Sydney Basin during the Wuchiapingian.

Unidirectional aridification during the Lopingian, and a shift in fluvial style from high-sinuosity to low-sinuosity across the EPE receive less support from the compilation of stratigraphic and geochemical evidence presented herein. Furthermore, while soil erosion in the Anthropocene is a very real danger, soil erosion during the Lopingian was ubiquitous without clear evidence of an increase in volume or reliable correlations during the EPE between the studied basins. A purported decrease in paleoatmospheric O2 during the EPE, however, has not received significant evidence that supports or refutes this hypothesis in this compilation of data. Rather, alternative hypotheses are raised herein to assess whether reducing conditions observed in the Karoo, Lebombo, and Transantarctic basins are related to basin-specific groundwater geochemistry or a global reduction in tropospheric O2 concentration. Ultimately, terrestrial ecosystems on Gondwana underwent transformation and extinction during the EPE of varying severity and timing, perhaps related to a single forcing (e.g., Siberian Traps volcanism). This review, however, highlights that significantly different responses to a single forcing can occur over a broad area, and that expectations of a unified hemispheric response to a given forcing (e.g., aridification, shift in fluvial style) were unlikely during the Late Permian.

Declaration of Competing Interest

The authors declare that they have no known competing financial interests or personal relationships that could have appeared to influence the work reported in this paper.

Acknowledgements

Earlier versions of this manuscript benefited from the comments of reviewer Dr. Robert Gastaldo, an anonymous reviewer, and Editor Dr. Thomas Algeo. This research was supported by National Science Foundation grants OISE 1559231, OPP 1443557 and OPP 1142749 to ELG.

Appendix A. Supplementary data

Supplementary data to this article can be found online at https://doi.org/10.1016/j.palaeo.2021.110762.

References

- Abdala, F., Dias-da-Silva, S., Cisneros, J.C., 2002. First record of non-mammalian cynodonts (Therapsida) in the Sanga do Cabral Formation (Early Triassic) of southern Brazil. Palaeontol. Afr. 38, 92–97.
- Alessandretti, L., Machado, R., Warren, L.V., Assine, M.L., Lana, C., 2016. From source-to-sink: the late Permian SW Gondwana paleogeography and sedimentary dispersion unrayeled by a multi-proxy analysis. J. S. Am. Farth Sci. 70, 368–382.
- Almeida, I.C.C., Schafer, C.G.R., Fernandes, R.B.A., Pereira, T.T.C., Nieuwendam, A., Pereira, A.B., 2014. Active layer thermal regime at different vegetation covers at Lions Rump, King George Island, Maritime Antarctica. Geomorphology 225, 36–46.
- Alonso-Zarza, A.M., Wright, V.P., Calvo, J.P., Garcia del Cura, M.A., 1992. Soil-landscape and climatic relationships in the middle Miocene of the Madrid Basin. Sedimentology 39, 17–35.
- Amit, R., Enzel, Y., Crouvi, O., 2020. Quaternary influx of proximal coarse-grained dust altered circum-Mediterranean soil productivity and impacted early human culture. Geology 49, 61–65.

- Archangelsky, S., 1992. Dictyopteridium feistmantel (fructificiation pérmica de glossopteridales): primer registro argentino. In: VII Simposio Argentino de Paleobotánica y Palinologia, 2. Publicación Especial de la Asosciación Paleontológica Argentina, pp. 19–22.
- Archangelsky, S., Cúneo, N.R., 2002. Floras del Paleozoic superior. Cuenca La Golondrina. In: Haller, M.J. (Ed.), Geología y Recursos Naturales de Santa Cruz, 15° Congreso Geológico Argentino (El Calafate), Relatorio, pp. 401–405.
- Aristov, D.S., Prevec, R., Mostovski, M.B., 2009. New and poorly known grylloblattids (Insecta: Grylloblattida) from the Lopingian of the Lebombo Basin, South Africa. Afr. Invertebr. 50, 279–286.
- Ashley, G.A., Driese, S.G., 2000. Paleopedology and paleohydrology of a volcaniclastic paleosol interval: implications for early Pleistocene stratigraphy and paleoclimate record, Olduvai Gorge, Tanzania. J. Sediment. Res. 70, 1065–1080.
- Askin, R.A., 1995. Permian palynomorphs from southern Victoria Land, Antarctica. Antarctic J. U.S. 30, 47–48.
- Barbolini, N., Bamford, M.K., Rubidge, B., 2016. Radiometric dating demonstrates that Permian spore-pollen zones of Australia and South Africa are diachronous. Gondwana Res. 37, 241–251.
- Barbolini, N., Rubidge, B., Bamford, M.K., 2018. A new approach to biostratigraphy in the Karoo retroarc foreland system: Utilising restricted-range palynomorphs and their first appearance datums for correlation. J. Afr. Earth Sci. 140, 114–133.
- Barrett, P.J., 1969. Stratigraphy and Petrology of the Mainly Fluviatile Permian and Triassic Beacon Rocks, Beardmore Glacier Area, Antarctica. Research Foundation and the Institute of Polar Studies, The Ohio State University.
- Barrett, P.J., Elliot, D.H., Lindsay, J.F., 1986. The Beacon Supergroup (Devonian–Triassic) and Ferrar Group (Jurassic) in the Beardmore Glacier area, Antarctica. In: Turner, M.D., Splettstoesser, J.F. (Eds.), Geology of the Central Transantarctic Mountains, American Geophysical Union, Antarctic Research Series, vol. 36, pp. 339–428.
- Beattie, R., 2007. The geological setting and palaeoenvironmental and palaeoecological reconstructions of the Upper Permian insect beds at Belmont, New South Wales, Australia. Afr. Invertebr. 48, 41–57.
- Bercovici, A., Cui, Y., Forel, M.B., Yu, J., Vajda, V., 2015. Terrestrial paleoenvironment characterization across the Permian-Triassic boundary in South China. J. Asian Earth Sci. 98, 225–246.
- Besly, B.M., Fielding, C.R., 1989. Palaeosols in Westphalian coal-bearing and red-bed sequences, central and northern England. Palaeogeogr. Palaeoclimatol. Palaeoecol. 70, 303–330.
- Bhattacharyya, D.P., 1983. Origin of berthierine in ironstones. Clay Clay Miner. 31, 173–182.
- Bordy, E.M., Prevec, R., 2008. Sedimentology, palaeontology and palaeo-environments of the Middle (?) to Upper Permian Emakwezini Formation (Karoo Supergroup, South Africa). S. Afr. J. Geol. 111, 429–458.
- Bordy, E.M., Sztanó, O., Rubidge, B.S., Bumby, A., 2011. Early Triassic vertebrate burrows from the Katberg Formation of the South-Western Karoo Basin, South Africa. Lethaia 44, 33–45.
- Botha, J., Smith, R.M.H., 2007. Lystrosaurus species composition across the Permo-Triassic boundary in the Karoo Basin of South Africa. Lethaia 40, 125–137. https:// doi.org/10.1111/j.1502-3931.2007.00011.x.
- Bown, T.M., Kraus, M.J., 1987. Integration of channel and floodplain suites; I, Developmental sequence and lateral relations of alluvial Paleosols. J. Sediment. Res. 57 (4), 587–601.
- Brennecka, G.A., Hermann, A.D., Algeo, T.J., Anbar, A.D., 2011. Rapid expansion of oceanic anoxia immediately before the end-Permian mass extinction. Proc. Natl. Acad. Sci. 108, 17631–17634.
- Briggs, D.E.G., Miller, M.F., Isbell, J.L., Sidor, C.A., 2010. Permo-Triassic arthropod trace fossils from the Beardmore Glacier area, central Transantarctic Mountains, Antarctica, Antarct. Sci. 22, 185–192.
- Bryan, K., Albritton, C.C., 1943. Soil phenomena as evidence of climatic changes. Am. J. Sci. 241 (8), 469–490.
- Cariglino, B., 2013. Fructification diversity from the La Golondrina Formation (Permian), Santa Cruz Province, Argentina. Geobios 46, 183–193.
- Cariglino, B., 2018. Patterns of insect-mediated damage in a Permian Glossopteris flora from Patagonia (Argentina). Palaeogeogr. Palaeoclimatol. Palaeoecol. https://doi. org/10.1016/j.palaeo.2018.06.022.
- Cascales-Miñana, B., Cleal, C.J., 2014. The plant fossil record reflects just two great extinction events. Terra Nova 26, 195–200.
- Cascales-Miñana, B., Diez, J.B., Gerrienne, P., Cleal, C.J., 2016. A palaeobotanical perspective on the great end-Permian biotic crisis. Hist. Biol. 28, 1066–1074.
- Chan, M.A., Parry, W.T., Bowman, J.R., 2000. Diagenetic hematite and manganese oxides and fault related fluid flow in Jurassic sandstones, southeastern Utah. AAPG Bull. 84, 1281–1310.
- Chan, M.A., Bowen, B.B., Parry, W.T., Ormö, J., Komatsu, G., 2005. Red rock and red planet diagenesis: comparisons of earth and mars concretions. GSA Today 15. https://doi.org/10.1130/1052-5173(2005)015<4:RRARPD>2.0.CO;2.
- Chu, D., Tong, J., Benton, M.J., Yu, J., Huang, Y., 2019. Mixed continental-marine biotas following the Permian-Triassic mass extinction in South and North China. Palaeogeogr. Paleoclimatol. Paleoecol. 519, 95–107.
- Cisneros, J.C., Abdala, F., Malabarba, M.C., 2005. Pareiasaurids from the Rio do Rasto Formation, southern Brazil: biostratigraphic implications for Permian faunas of the Paraná Basin. Rev. Brasil. Paleontol. 8, 13–24.
- Collinson, J.W., Isbell, J.L., Elliot, D.H., Miller, M.F., Miller, J.M.G., 1994.

 Permian–Triassic Transantarctic Basin. In: Veevers, J.J., Powell, C.McA (Eds.),

 Permian–Triassic Pangean Basins and Foldbelts along the Panthalassan Margin of
 Gondwanaland, 184. Geological Society of America Memoir, pp. 173–222.

- Collinson, J.W., 1990. Depositional setting of late carboniferous to Triassic biota in the Transantarctic Basin. In: Antarctic Paleobiology. Springer, New York, NY, pp. 1–14.
- Collinson, J.W., Hammer, W.R., Askin, R.A., Elliot, D.H., 2006. Permian-Triassic boundary in the central Transantarctic Mountains, Antarctica. Geol. Soc. Am. Bull. 118, 747–763.
- Collinson, J.W., Kemp, N.R., Eggert, J.T., 1987. Comparison of the Triassic Gondwana sequences in the Transantarctic Mountains and Tasmania. American Geophysical Union, pp. 51–61.
- Coney, L., Reimold, W.U., Hancox, J.P., Mader, D., Koeberl, C., McDonald, I., Stuck, U., Vajda, V., Kamo, S.L., 2007. Geochemical and mineralogical investigations of the Permian-Triassic boundary in the continental realm of the southern Karoo Basin, South Africa. Paleoworld 16, 67–104. https://doi.org/10.1016/l.palwor.2007.05.003.
- Cui, Y., Kump, L.R., 2015. Global warming and the end-Permian extinction event: Proxy and modeling perspectives. Earth Sci. Rev. 149, 5–22.
- Cúneo, N.R., Isbell, J., Taylor, E.L., Taylor, T.N., 1993. The Glossopteris flora from Antarctica: taphonomy and paleoecology. In: Comptes Rendux XII International Congress for the Carboniferous and Permian, Buenos Aires, 2, pp. 13–40.
- Cúneo, N.R., Taylor, E.L., Taylor, T.N., Krings, M., 2003. In situ fossil forest from the upper Fremouw Formation (Triassic) of Antarctica: paleoenvironmental setting and paleoclimate analysis. Palaeogeogr. Palaeoclimatol. Palaeoecol. 197, 239–261.
- Dalziel, I.W., Elliot, D.H., 1982. West Antarctica: problem child of Gondwanaland. Tectonics 1 (1), 3–19.
- Day, M., Ramezani, J., Bowring, S., Sadler, P., Erwin, D., Abdala, F., Rubidge, B., 2015.
 When and how did the terrestrial mid-Permian mass extinction occur? Evidence from the tetrapod record of the Karoo Basin, South Africa. Proc. R. Soc. B 282, 20150834.
- de Santa Ana, H., Veroslavsky, G., Fulfaro, V., Rossello, E., 2006. Cuenca Norte: evolución tectónica y sedimentaria del Carbonífero–Pérmico. In: Veroslavsky, G., Ubilla, M., Martínez, S. (Eds.), Cuencas Sedimentarias de Uruguay. División Relaciones y Actividades Culturales Facultad de Ciencias, Montevideo, pp. 147–208.
- Decombeix, A.-L., Taylor, E.L., Taylor, T.N., 2009. Secondary growth in Vertebraria roots from the late Permian of Antarctica: a change in developmental timing. Int. J. Plant Sci. 170, 644–656.
- Decombeix, A.-L., Durieux, T., Harper, C.J., Serbet, R., Taylor, E.L., 2021. A Permian nurse log and evidence for facilitation in high-latitude *Glossopteris* forests. Lethaia 54, 96–105.
- Dias, K.D.N., Scherer, C.M.S., 2008. Cross-bedding set thickness and stratigraphic architecture of aeolian systems: an example from the Upper Permian Pirambóia Formation (Paraná Basin), southern Brazil, J. S. Am. Earth Sci. 25, 405–415.
- Dias-da-Silva, S., 2012. Middle-Late Permian tetrapods from the Rio do Rasto Formation, Southern Brazil: a biostratigraphic reassessment. Lethaia 45, 109–120.
- Driese, S.G., Mora, C.I., Stiles, C.A., Joeckel, R.M., Nordt, L.C., 2000. Mass-balance reconstruction of a modern Vertisol: implications for interpreting the geochemistry and burial alteration of paleo-Vertisols. Geoderma 95, 179–204.
- Driese, S.G., Nordt, L.C., Lynn, W.C., Stiles, C.A., Mora, C.I., Wilding, L.P., 2005.
 Distinguishing climate in the soil record using chemical trends in a Vertisol climosequence from the Texas Coast Prairie, and application to interpreting Paleozoic paleosols in the Appalachian Basin, U.S.a. J. Sediment. Res. 75, 339–349.
- Dzombak, R.M., Sheldon, N.D., 2020. Weathering intensity and presence of vegetation are key controls on soil phosphorus concentrations: implications for past and future terrestrial ecosystems. Soil Syst. 4, 73. https://doi.org/10.3390/soilsystems4040073.
- Dzombak, R.M., Sheldon, N.D., Mohabey, D.M., Samant, B., 2020. Stable climate in India during Deccan volcanism suggests limited influence on K-Pg extinction. Gondwana Res. GR238 https://doi.org/10.1016/j.gr.2020.04.007.
- Dzombak, R.M., Midttun, N.C., Stein, R.A., Sheldon, N.D., 2021. Incorporating lateral variability and extent of paleosols into proxy uncertainty. Palaeogeogr. Palaeoclimatol. Palaeoecol.
- Ekart, D.D., Cerling, T.E., Montañez, I.P., Tabor, N.J., 1999. A 400 million year carbon isotopic record of pedogenic carbonate: implications for paleoatmospheric carbon dioxide. Amer. J. Sci. 299, 805–827.
- Elliot, D.H., Fanning, C.M., Isbell, J.L., Hulett, S.R.W., 2017. The Permo-Triassic Gondwana sequence, central Transantarctic Mountains, Antarctica: Zircon geochronology, provenance, and basin evolution. Geosphere 13, 155–178.
- Ernesto, M., Demarco, P.N., Xavier, P., Sanchez, L., Schultz, C., Piñeiro, G., 2020. Age constraints on the Paleozoic Yaguarí-Buena Vista succession from Uruguay: paleomagnetic and paleontologic information. J. S. Am. Earth Sci. 98, 102489.
- Erwin, D.H., 1994. The Permo-Triassic extinction. Nature 367, 231–235.
- Farabee, M.J., Taylor, E.L., Taylor, T.N., 1990. Correlation of Permian and Triassic palynomorph assemblages from the central Transantarctic Mountains, Antarctica. Rev. Palaeobot. Palynol. 65, 257–265.
- Fielding, C.R., Alexander, J., 2001. Fossil trees in ancient fluvial channel deposits: evidence of seasonal and longer-term climatic variability. Palaeogeogr. Palaeoclimatol. Palaeoecol. 170, 59–80.
- Fielding, C.R., Webb, J.A., 1996. Facies and cyclicity of the late Permian Bainmedart Coal measures in the Northern Prince Charles Mountains, MacRobertson Land, Antarctica. Sedimentology 43, 295–322.
- Fielding, C.R., Frank, T.D., Birgenheier, L.P., Rygel, M.C., Jones, A.T., Roberts, J., 2008. Stratigraphic imprint of the late Paleozoic Ice Age in eastern Australia: a record of alternating glacial and nonglacial climate regime. Geol. Soc. London J. 165, 129-140
- Fielding, C.R., Alexander, J., Allen, J.P., 2018. The role of discharge variability in the formation and preservation of alluvial sediment bodies. Sediment. Geol. https://doi. org/10.1016/j.sedgeo.2017.12.022.
- Fielding, C.R., Frank, T.D., McLoughlin, S., Vajda, V., Mays, C., Tevyaw, A.P., Winguth, A., Winguth, C., Nicoll, R.S., Bocking, M., Crowley, J.L., 2019. Age and

- pattern of the southern high-latitude continental end-Permian extinction constrained by multiproxy analysis. Nat. Commun. 10, 385.
- Fielding, C.R., Frank, T.D., Tevyaw, A.P., Savatic, K., Vajda, V., McLoughlin, S., Mays, C., Nicoll, R.S., Bocking, M., Crowley, J.L., 2021. Sedimentology of the continental end-Permian extinction event in the Sydney Basin, eastern Australia. Sedimentology 68, 30–62
- Fildani, A., Drinkwater, N.J., Weislogel, A., McHargue, T., Hodgson, D.M., Flint, S.S., 2007. Age controls on the Tanqua and Lainsburg deep-water systems: new insights on the evolution and sedimentary fill of the Karoo Basin, South Africa. J. Sediment. Res. 77. 901–908.
- Fildani, A., Weislogel, A., Drinkwater, N.J., McHargue, T., Tankard, A., Wooden, J., Hodgson, D., Flint, S.S., 2009. U-Pb zircon ages from the southwestern Karoo Basin, South Africa-implications for the Permian-Triassic boundary. Geology 37, 719–722.
- Fitzgerald, P.G., Barret, P.J., 1986. Skolithos in a Permian braided river deposit, southern Victoria Land, Antarctica. Palaeogeogr. Palaeoclimatol. Palaeoecol. 52, 237–247.
- Francischini, H., Dentzien-Dias, P., Guerra-Sommer, M., Menegat, R., Santos, J.O.S., Manfroi, J., Schultz, C.L., 2018a. A Middle Permian (Roadian) lungfish aestivation burrow from the Rio do Rasto Formation (Paraná Basin, Brazil) and associated U-Pb dating. Palaios 33, 69–84.
- Francischini, H., Dentzien-Dias, P., Lucas, S.G., Schultz, C.L., 2018b. Tetrapod tracks in Permo–Triassic eolian beds of southern Brazil (Paraná Basin). Peer J. 6, e4764 doi.10.7717/peerj.4764.
- Frank, T.D., Fielding, C.R., Winguth, A.M.E., Savatic, K., Tevyaw, A., Winguth, C., McLoughlin, S., Vajda, V., Mays, C., Nicoll, R., Bocking, M., Crowley, J.L., 2021. Pace, magnitude, and nature of terrestrial climate change through the end-Permian extinction in southeastern Gondwana. Geology 49 doi.10.1130/G487951.
- Gallagher, T.M., Sheldon, N.D., 2013. A new paleothermometer for forest paleosols and its implications for Cenozoic climate. Geology 41, 647–650.
- Gallagher, T.M., Hren, M., Sheldon, N.D., 2019. The effect of soil temperature seasonality on climate reconstructions from paleosols. Am. J. Sci. 319, 549–581.
- Gastaldo, R.A., 2010. Peat or no peat: why do the Rajang and Mahakam Deltas differ? Int. J. Coal Geol. 83, 162–172.
- Gastaldo, R.A., Demko, T.M., 2011. The relationship between continental landscape evolution and the plant-fossil record: long term hydrology controls and the plant-fossil record: long term hydrology controls on preservation. In: Allison, P.A., Bottjer, D.J. (Eds.), Taphonomy. Aims & Scope Topics in Geobiology Book Series, v. 32. Springer, Dordrecht. https://doi.org/10.1007/978-90-481-8643-37.
- Gastaldo, R.A., Rolerson, M.W., 2008. Katbergia gen. nov., A new trace fossil from the Upper Permian and lower Triassic rocks of the Karoo Basin: implications for paleoenvironmental conditions at the P/Tr extinction event. Palaeontology 51, 215–229.
- Gastaldo, R.A., Neveling, J., Clark, K., Newbury, S.S., 2009. The terrestrial Permian-Triassic boundary event bed is a nonevent. Geology 37, 199–202.
- Gastaldo, R.A., Neveling, J., Looy, C.V., Bamford, M.K., Kamo, S.L., Geissman, J.W., 2017. Paleontology of the Blaauwater 67 and 65 farms, South Africa: testing the daptocephalus/lystrosaurus biozone boundary in a stratigraphic framework. Palaios 32 (6), 349–366. https://doi.org/10.2110/palo.2016.106.
- Gastaldo, R.A., Pludow, B.A., Neveling, J., 2013. Mud aggregates from the Katberg Formation, South Africa: additional evidence for Early Triassic degradational landscapes. J. Sediment. Res. 83, 531–540.
- Gastaldo, R.A., Knight, C.L., Neveling, J., Tabor, N.J., 2014. Latest Permian paleosols from Wapadsberg Pass, South Africa: Implications for Changhsingian climate. GSA Bull. 126, 665–679.
- Gastaldo, R.A., Kamo, S.L., Neveling, J., Geissman, J.W., Bamford, M., Looy, C.V., 2015. Is the vertebrate-defined Permian-Triassic boundary in the Karoo Basin, South Africa, the terrestrial expression of the end-Permian marine event? Geology 43, 939–942.
- Gastaldo, R.A., Neveling, J., Geissman, J.W., Kamo, S.L., 2018. A lithostratigraphic and magnetostratigraphic framework in a geochronologic context for a purported Permian–Triassic boundary section at Old (West) Lootsberg Pass, Karoo Basin, South Africa. GSA Bull. 130, 1411–1438. https://doi.org/10.1130/B31881.1.
- Gastaldo, R.A., Neveling, J., Geissman, J.W., Looy, C.V., 2019. Testing the *Daptocephalus* and *Lystrosaurus* Assemblage zones in a lithostratigraphic, magnetostratigraphic, and palynological framework in the Free State, South Africa. Palaios 34, 542–561.
- Gastaldo, R.A., Kus, L., Tabor, N.J., Neveling, J., 2020a. Calcic Vertisols in the upper Daptocephalus Assemblage Zone, Balfour Formation, Karoo Basin, South Africa for late Permian climate. J. Sediment. Res. v., p.
- Gastaldo, R.A., Kamo, S.L., Neveling, J., Geissman, J.W., Looy, C.V., Martini, A.M., 2020b. The base of the Lystrosaurus Assemblage Zone, Karoo Basin, predates the end-Permian marine extinction. Nat. Commun. 11, 1428. https://doi.org/10.1038/ s41467-020-15243-7.
- Gastaldo, R.A., Tabor, N.J., Neveling, J., 2020c. Trends in stable isotopes and climate proxies from late Changhsingian ghost landscapes of the Karoo Basin, South Africa. Front. Ecol. Evol. 8, 567109 https://doi.org/10.3389/fevo.2020.567109.
- Gastaldo, R.A., Neveling, J., Geissman, J.W., Kamo, S.L., Looy, C.V., 2021. A tale of two Tweefonteins: what physical correlation, geochronology, magnetic polarity stratigraphy, and palynology reveal about the end-Permian terrestrial extinction paradigm in South Africa. GSA Bull. https://doi.org/10.1130/B35830.1.
- Ghosh, P., Garzione, C.N., Eiler, J.M., 2006. Rapid uplift of the Altiplano revealed through ¹³C-¹⁸O bonds in paleosol carbonates. Science 311 (5760), 511–515.
- Gile, L.H., Grossman, R.B., 1968. Morphology of the argillic horizon in desert soils of southern New Mexico. Soil Sci. 106, 6–15.
- Goldberg, K., Humayun, M., 2010. The applicability of the Chemical Index of Alteration as a paleoclimatic indicator: an example from the Permian of the Paraná Basin, Brazil. Palaeogeogr. Palaeoclimatol. Palaeoecol. 293, 175–183.

- Goso, C., Piñeiro, G., de Santa Ana, H., Rojas, A., Verde, M., Alves, C., 2001.
 Caracterización estratigráfica de los depósitos continentals cuspidales neopérmicos (Formaciones Yaguarí y Buena Vista) en el borde oriental de la Cuenca Norte Uruguaya. Actas, XI Congreso Latinoamericano de Geología, p. 18.
- Grasby, S.E., Beauchamp, B., 2009. Latest Permian to early Triassic basin-to-shelf anoxia in the Sverdrup Basin, Arctic Canada. Chem. Geol. 264, 232–246.
- Grime, J.P., 1977. Evidence for the existence of three primary strategies in plants and its relevance to ecological and evolutionary theory. Am. Nat. 111, 1169–1194.
- Grittinger, T.F., 1970. String bog in southern Wisconsin. Ecology 51, 928–930.
- Gulbranson, E.L., Montañez, I.P., Tabor, N.J., 2011. A proxy for humidity and floral province from paleosols. J. Geol. 119, 559–573.
- Gulbranson, E.L., Isbell, J.L., Taylor, E.L., Ryberg, P.E., Taylor, T.N., Flaig, P.P., 2012.
 Permian polar forests: deciduousness and environmental variation. Geobiology 10, 479–495.
- Gulbranson, E.L., Ryberg, P.E., Decombeix, A.-L., Taylor, E.L., Taylor, T.N., Isbell, J.L., 2014. Leaf habit of late Permian Glossopteris trees from high-palaeolatitude forests. J. Geol. Soc. 171, 493–507.
- Gulbranson, E.L., Montañez, I.P., Tabor, N.J., Limarino, C.O., 2015a. Late Pennsylvanian aridification on the southwestern margin of Gondwana (Paganzo Basin, NW Argentina): a regional expression of a global climate perturbation. Palaeogeogr. Palaeoclimatol. Palaeoecol. 417, 220–235.
- Gulbranson, E.L., Ciccioli, P.L., Montañez, I.P., Marenssi, S.A., Limarino, C.O., Schmitz, M.D., Davydov, V., 2015b. Paleoenvironments and age of the Talampaya Formation: the Permo-Triassic boundary in northwestern Argentina. J. S. Am. Earth Sci. 63, 310–322.
- Gulbranson, E.L., Cornamusini, G., Ryberg, P.E., Corti, V., 2020. When does large woody debris influence ancient rivers? Dendrochronology applications in the Permian and Triassic, Antarctica. Palaeogeogr. Palaeoclimatol. Palaeoecol. v., p.
- Gunal, H., Ransom, M.D., 2006. Clay illuviation and calcium carbonate accumulation along a precipitation gradient in Kansas. Catena 68, 59–69.
- Gutiérrez, P.R., Zavattieri, A.M., Noetinger, S., 2018. The Lopingian palynological Guttulapollenites hannonicus—Cladaitina veteadensis assemblage zone of Argentina, stratigraphical implications for Gondwana. J. S. Am. Earth Sci. 88, 673–692.
- Hancox, P.J., Neveling, J., Rubidge, B.S., 2020. Biostratigraphy of the Cynognathus Assemblage Zone (Beaufort Group, Karoo Supergroup), South Africa. S. Afr. J. Geol. 123, 217–238. https://doi.org/10.25131/sajg..123.0016.
- Hartley, A.J., Weissmann, G.S., Bhattacharayya, P., Nichols, G.J., Scuderi, L.A.,
 Davidson, S.K., Leleu, S., Chakraborty, T., Parthasarathi, G., Mather, A.E., 2013. Soil development on modern distributive fluvial systems: preliminary observations with implications for interpretation of paleosols in the rock record. In: Driese, S.G.,
 Nordt, L.C., McCarthy, P.J. (Eds.), In: New Frontiers in Paleopedology and Terrestrial Paleoclimatology-Paleosols and Soil Surface Analog Systems. SEPM Special Publication. No. 104, p. 149–158.
- Heinselman, M.L., 1965. String bogs and other patterned organic terrain near Seney, Upper Michigan. Ecology 46, 185–188.
- Herbert, C., 1997. Relative Sea level control of deposition in the late Permian Newcastle Coal measures of the Sydney Basin, Australia. Sediment. Geol. 107, 167–187.
- Holz, M., França, A.B., Souza, P.A., Iannuzzi, R., Rohn, R., 2010. A stratigraphic chart of the late Carboniferous/Permian succession of the eastern border of the Paraná Basin, South America. J. S. Am. Earth Sci. 29, 381–399.
- Horton, D.E., Poulsen, C.J., Montañez, I.P., DiMichele, W.A., 2012. Eccentricity-paced late Paleozoic climate change. Palaeogeogr. Palaeoclimatol. Palaeoecol. 331–332, 150–161.
- Hotinski, R.M., Bice, K.L., Kump, L.R., Najjar, R.G., Arthur, M.A., 2001. Ocean stagnation and end-Permian anoxia. Geology 29, 7–10.
- Huey, R.B., Ward, P.D., 2005. Hypoxia, global warming, and terrestrial late Permian extinctions. Science 308 (5720), 398–401.
- Iannuzzi, R., 2010. The flora of early Permian coal measures from the Paraná Basin in Brazil: a review. Int. J. Coal Geol. 83, 229–247.
- Iljima, A., Matsumoto, R., 1982. Berthierine and chamosite in coal measures of Japan. Clay Clay Miner. 30, 264–274.
- Isbell, J.L., 1991. Evidence for a low-gradient alluvial fan from the palaeo-Pacific margin in the Upper Permian Buckley Formation, Beardmore. Geolog. Evol. Antarct. 1, 215.
- Isbell, J.L., Cúneo, N.R., 1996. Depositional framework of Permian coal-bearing strata, southern Victoria Land, Antarctica. Palaeogeogr. Palaeoclimatol. Palaeoecol. 125, 217–238.
- Jin, Y.G., Wang, Y., Wang, E., Shang, Q.H., Cao, C.Q., Erwin, D.H., 2000. Pattern of marine mass extinction near the Permian–Triassic boundary in South China. Science 289, 432–436.
- Kaiho, K., Aftabuzzaman, Md., Jones, D.S., Tian, L., 2020. Pulsed volcanic combustion events coincident with the end-Permian terrestrial disturbance and the following global crisis. Geology 49 doi.10.1130/G48022.1.
- Khormali, F., Abtahi, A., Mahmoodi, S., Stoops, G., 2003. Argillic horizon development in calcareous soils of arid and semiarid regions of southern Iran. Catena 53, 273–301
- Kiehl, J.T., Shields, C.A., 2005. Climate simulation of the latest Permian: implications for mass extinction. Geology 33, 757–760. https://doi.org/10.1130/G21654.1.
- King, G.M., Cluver, M.A., 1991. The aquatic Lystrosaurus: an alternative lifestyle. Hist. Biol. 4, 323–342.
- Kocurek, G., Fielder, G., 1982. Adhesion structures. J. Sediment. Petrol. 51, 1229–1241.
 Kocurek, G., Lancaster, N., 1999. Aeolian system sediment state: theory and Mojave Desert Kelso dune field example. Sedimentology 46, 505–515.
- Kraus, M.J., 1999. Paleosols in clastic sedimentary rocks: their geologic applications. Earth Sci. Rev. 47, 41–70.
- Kraus, M.J., 2002. Basin-scale changes in floodplain paleosols: implications for interpreting alluvial architecture. J. Sediment. Res. 72, 500–509.

- Kraus, M.J., Aslan, A., 1993. Eocene hydromorphic palaoeols; significance for
- interpreting ancient floodplain processes. J. Sediment. Res. 63, 453–463. Krull, E.S., Retallack, G.J., 2000. 8¹³C depth profiles from paleosols across the Permian-Triassic boundary: evidence for methane release. Geol. Soc. Am. Bull. 112, 1459–1472.
- Kyle, R.A., Schopf, J.M., 1982. Permian and Triassic palynostratigraphy of the Victoria Group, Transantarctic Mountains. In: Craddock, C. (Ed.), Antarctic Geosciences. University of Wisconsin Press, Madison, pp. 649–659.
- La Prade, K.E., 1982. Petrology and petrography of the Beacon Supergroup, Shackleton Glacier area, Queen Maude Range, Transantarctic Mountains, Antarctica. In: Craddock, C. (Ed.), Antarctic Geoscience: Madison, University of Wisconsin Press, International Union of Geological Sciences, Series B-4, pp. 581–590.
- Lancaster, N., 1992. Relations between dune generations in the Gran Desierto of Mexico. Sedimentology 36, 631–644.
- Lanci, L., Tohver, E., Wilson, A., Flint, S., 2013. Upper Permian magnetic stratigraphy of the lower Beaufort Group, Karoo Basin. Earth Planet. Sci. Lett. 375, 123–134.
- Laurie, J.R., Bodorkos, S., Nicoll, R.S., Crowley, J.L., Mantle, D.J., Mory, A.J., Wood, G. R., Backhouse, J., Holmes, E.K., Smith, T.E., Champion, D.C., 2016. Calibrating the middle and late Permian palynostratigraphy of Australia to the geologic time-scale via U-Pb zircon CA-IDTIMS dating. Aust. J. Earth Sci. 63, 701–730.
- Lavina, E.L.C., Faccini, U.F., Ribeiro, H.J.S., 1993. A Formação Pirambóia (Permotriássico) no estado do Rio Grande do Sul. Acta Geol. Leopold. 38, 179–197.
- Lenton, T.M., Daines, S.J., Mills, B.J.W., 2018. COPSE reloaded: an improved model of biogeochemical cycling over Phanerozoic time. Earth Sci. Rev. 178, 1–28.
- Li, J., Gastaldo, R.A., Neveling, J., Geissman, J.W., 2017. Siltstones across the Daptocephalus (Dicynodon) and Lystrosaurus Assemblage zones, Karoo Basin, South Africa, show no evidence for aridification. J. Sediment. Res. 87, 653–671.
- Liberato, G.P., Cornamusini, G., Perotti, M., Sandroni, S., Talarico, F.M., 2017. Stratigraphy of a Permian-Triassic fluvial-dominated succession in Southern Victoria Land (Antarctica): preliminary data. J. Mediterranean Earth Sci. 9, 167–171.
- Lieth, H., 1975. Primary production of the major vegetation units of the world. In: Lieth, H., Whitaker, R.H. (Eds.), Primary Productivity of the Biosphere. Springer, New York, pp. 203–215.
- Limarino, C.O., Spalletti, L.A., 2006. Paleogeography of the upper Paleozoic basins of southern South America: an overview. J. S. Am. Earth Sci. 22, 134–155.
- Limarino, C.O., Césari, S.N., Spalletti, L.A., Taboada, A.C., Isbell, J.L., Geuna, S., Gulbranson, E.L., 2014. A paleoclimatic review of southern South America during the late Paleozoic: a record from icehouse to extreme greenhouse conditions. Gondwana Res. 25, 1396–1421.
- Lindbo, D.L., 1997. Entisols-fluvents and fluvaquents: Problems recognizing aquic and hydric conditions in young, flood plain soils. In: Vepraskas, M.J., Sprecher, S.W. (Eds.), Aquic Conditions and Hydric Soils: The Problem Soils, vol. 50. SSSA Special Publication, pp. 133–151.
- Liu, H.-Y., Wei, H.-B., Chen, J., Guo, Y., Zhou, Y., Gou, X.-D., Yang, S.-L., Labandeira, C., Feng, Z., 2021. A Latitudinal Gradient of Plant-Insect Interactions during the Late Permian in Terrestrial Ecosystems? Global and Planetary Change, doi, New evidence from Southwest China. https://doi.org/10.1016/j.gloplacha.2020.103248.
- Lukens, W.E., Nordt, L.C., Stinchcomb, G.E., Driese, S.G., Tubbs, J.D., 2018.Reconstructing pH of paleosols using geochemical proxies. J. Geol. 126, 427–449.
- Mack, G.H., James, W.C., Monger, H.C., 1993. Classification of paleosols. Geol. Soc. Am. Bull. 105. 129–136.
- Malabarba, M.C., Abdala, F., Weiss, F.E., Perez, P.A., 2003. New data on the late Permian vertebrate fauna of Posto Quimado, Rio do Rasto Formation, southern Brazil. Rev. Brasil. Paleontol. 6, 49–54.
- Martinelli, A.G., Francischini, H., Dentzien-Dias, P., Soares, M.B., Schultz, C.L., 2017. The oldest archosauromorph from South America: postcranial remains from the Guadalupian (mid-Permian) Rio do Rasto Formation (Paraná Basin), southern Brazil. Hist. Biol. 29, 76–84.
- Maynard, J.B., 1992. Chemistry of modern soils as a guide to interpreting Precambrian paleosols. J. Geol. 100, 279–289.
- Mays, C., Vajda, V., Frank, T.D., Fielding, C.R., Nicoll, R.S., Tevyaw, A.P., McLoughlin, S., 2019. Refined Permian–Triassic floristic timeline reveals early collapse and delayed recovery of south polar terrestrial ecosystems. GSA Bull. https://doi.org/10.1130/B35355.1.
 McDaniel, P.A., Graham, R.C., 1992. Organic carbon distribtions in shallow soils of
- McDaniel, P.A., Graham, R.C., 1992. Organic carbon distributions in shallow soils of Pinyon-Juniper woodlands. Soil Sci. Soc. Am. J. 56, 499–504.
- McDonald, E.V., Busacca, A.J., 1990. Interaction between aggrading geomorphic surfaces and the formation of a Late Pleistocene paleosol in the Palouse loess of eastern Washington state. In: Knuepfer, P.L.K., McFadden, L.D. (Eds.), Soils and Landscape Evolution. Geomorphology, v. 3, pp. 449–470.
- McLoughlin, S., 2011. Glossopteris-insights into the architecture and relationships of an iconic Permian Gondwanan plant. J. Botanical Soc. Bengal 65, 93–106.
- McLoughlin, S., Mays, C., Vajda, V., Bocking, M., Frank, T.D., Fielding, C.R., 2020.Dwelling in the dead zone Vertebrate burrows immediately succeeding the end-Permian extinction event in Australia. Palaios 35, 342–357.
- Metcalfe, I., 2013. Gondwana dispersion and Asian accretion: tectonic and palaeogeographic evolution of eastern Tethys. J. Asian Earth Sci. 66, 1–33.
- Metcalfe, I., Crowley, J.L., Nicoll, R.S., Schmitz, M., 2015. High-precision U-Pb CA-TIMS calibration of Middle Permian to lower Triassic sequences, mass extinction and extreme climate-change in eastern Australian Gondwana. Gondwana Res. 28, 61–81.
- Meyers, T.S., Tabor, N.J., Jacobs, L.L., Mateus, O., 2012. Estimating soil pCO_2 using paleosol carbonates: implications for the relationship between primary productivity and faunal richness in ancient terrestrial ecosystems. Paleobiology 38, 585–604.
- Michel, L.A., Tabor, N.J., Montañez, I.P., Schmitz, M.D., Davydov, V.I., 2015. Chronostratigraphy and paleoclimatology of the Lodève Basin, France: Evidence for

- a pan-tropical aridification event across the Carboniferous–Permian boundary. Palaeogeogr. Palaeoclimatol. Palaeoecol. 430, 118–131.
- Miller, M.F., Collinson, J.W., 1994. Trace fossils from Permian and Triassic sandy braided stream deposits, central Transantarctic Mountains. Palaios 9, 605–610.
- Miller, M.F., Knepprath, N.E., Cantrill, D.J., Francis, J.E., Isbell, J.L., 2016. Highly productive polar forests from the Permian of Antarctica. Palaeogeogr. Palaeoclimatol. Palaeoecol. v. 441 (part 2), 292–304.
- Minter, N.J., Buatois, L.A., Mángano, M.G., Davies, N.S., Gibling, M.R., Labandeira, C., 2016. The establishment of continental ecosystems. In: Mángano, M.G., Buatois, L.A. (Eds.), The Trace-Fossil Record of Major Evolutionary Events, Topics in Geobiology, 39. Springer. https://doi.org/10.1007/978-94-017-9600-2_6.
- Modesto, S.P., 2020. The disaster taxon Lystrosaurus: a paleontological myth. Front. Earth Sci. 8, 610463. https://doi.org/10.3389/feart.2020.610463.
- Modesto, S.P., Botha-Brink, J., 2010. A burrow cast with Lystrosaurus skeletal remains from the Lower Triassic of South Africa. Palaios 25 (4), 274–281.
- Montañez, I.P., 2013. Modern soil system constraints on reconstructing deep-time atmospheric CO₂. Geochim. Cosmochim. Acta 101, 57–75.
- Montañez, I.P., Tabor, N.J., Niemeier, D., DiMichele, W.A., Frank, T.D., Fielding, C.R., Isbell, J.L., Birgenheier, L.P., Rygel, M.C., 2007. CO₂-forced climate and vegetation instability during late Paleozoic deglaciation. Science 315, 87–91.
- Mora, C.I., Driese, S.G., Colarusso, L.A., 1996. Middle to late Paleozoic atmospheric CO₂ levels from soil carbonate and organic matter. Science 271, 1105–1107.
- Muhs, D.R., 2007. Paleosols and wind-blown sediments: Overview. In: Elias, S.A. (Ed.), Encyclopedia of Quaternary Science, Online Version. Elsevier, London, pp. 2075–2286.
- Mundil, R., Metcalfe, I., Chang, S., Renne, P.R., 2006. The Permian-Triassic boundary in Australia: New radio-isotopic ages. 16th Goldschmidt Conference Melbourne, Awards ceremony speeches and abstracts. Geochim. Cosmochim. Acta 70, A436.
- Neregato, R., Souza, P.A., Rohn, R., 2008. Registros palinológicos inéditos nas Formações Teresina e Rio do Rasto (Permian, Grupo, Passa Dois, Bacia do Paraná): implicações biocronoestratigráficas e paleoambientais. Pesq. Geoci 3, 9–21.
- Nordt, L.C., Driese, S.G., 2010. New weathering index improves paleorainfall estimates from Vertisols. Geology 38, 407–410.
- Nordt, L.C., Dworkin, S.I., Atchley, S.C., 2011. Ecosystem response to soil biogeochemical behavior during the late cretaceous and early Paleocene within the western interior of North America. GSA Bull. 123, 1745–1762.
- Nowak, H., Schneebeli-Hermann, E., Kustatscher, E., 2019. No mass extinction for land plants at the Permian-Triassic transition. Nat. Commun. 10, 384. https://doi.org/ 10.1038/s41467-018-07945-w.
- Oghenekome, M.E., Chatterjee, T.K., van Bever Donker, J.M., Hammond, N.Q., 2018. Geochemistry and weathering history of the Balfour sandstone formation, Karoo Basin, South Africa: Insight to provenance and tectonic setting. J. Afr. Earth Sci. 147, 623–632.
- Pace, D.W., Gastaldo, R.A., Neveling, J., 2009. Early Triassic aggradational and degradational landscapes of the Karoo Basin and evidence for climate oscillation following the P–Tr event. J. Sediment. Res. 79, 316–331.
- Pacheco, C.P., Eltink, E., Müller, R.T., Dias-da-Silva, S., 2016. A new Permian temnospondyl with Russian affinities from South America, the new family Konzhukoviidae, and the phylogenetic status of Archegosauroidea. J. Syst. Palaeontol. https://doi.org/10.1080/14772019.2016.1164763.
- Pal, D.K., Srivastava, P., Bhattacharyya, T., 2003. Clay illuviation in calcareous soils of the semiarid part of the Indo-Gangetic Plains, India. Catena 115, 177–192.
- Pankhurst, R.J., 2002. Marie Byrd Land, West Antarctica; Evolution of Gondwana's Pacific margin constrained by zircon U-Pb geochronology and feldspar common-Pb isotopic compositions: Discussion. Geol. Soc. Am. Bull. 114, 1178–1180.
- Passey, B.H., Levin, N.E., Cerling, T.E., Brown, F.H., Eiler, J.M., 2010. High-temperature environments of human evolution in East Africa based on bond ordering in paleosol carbonates. Proc. Natl. Acad. Sci. 107, 11245–11249.
- Pigg, K.B., McLoughlin, S., 1997. Anatomically preserved Glossopteris leaves from the Bowen and Sydney basins, Australia. Rev. Palaeobot. Palynol. 97, 339–359.
- Pigg, K.B., Taylor, T.N., 1993. Anatomically preserved Glossopteris stems with attached leaves from the central Transantarctic Mountains, Antarctica. Am. J. Bot. 80, 500–516
- Piñeiro, G., Marsicano, C., Lorenzo, N., 2007. A new temnospondyl from the Permo-Triassic Buena Vista Formation of Uruguay. Palaeontology 50, 627–640.
- Piñeiro, G., Ramos, A., Marsicano, C., 2012. A rhinesuchid-like temnospondyl from the Permo-Triassic of Uruguay. Comp. Rendus Palevol. 11, 65–78.
- Prevec, R., Labandeira, C.C., Neveling, J., Gastaldo, R.A., Looy, C.V., Bamford, M., 2009. Portrait of a Gondwanan Ecosystem: A New Late Permian Fossil Locality from KwaZulu-Natal. Review of Palaeobotany and Palynology, South Africa. https://doi. org/10.1016/j.revpalbo.2009.04.012.
- Prevec, R., Gastaldo, R.A., Neveing, J., Reid, S.B., Looy, C.V., 2010. An autochthonous glossopterid flora with latest Permian palynomorphs and its depositional setting in the *Dicynodon* Assemblage Zone of the southern Karoo Basin, South Africa. Palaeogeogr. Palaeoclimatol. Palaeoecol. 292, 391–408.
- Quade, J., Eiler, J., Daeron, M., Achyuthan, H., 2013. The clumped isotope geothermometer in soil and paleosol carbonate. Geochim. Cosmochim. Acta 105, 92–107.
- Rees, M.P., 2002. Land-plant diversity and the end-Permian mass extinction. Geology 30, 827–830.
- Reis, A.D.D., Scherer, C.M.D.S., Amarante, F.B.D., Roessetti, M.D.M.M., Kifumbi, C., de Souza, E.G., Ferronatto, J.P.F., Owen, A., 2019. Sedimentology of the proximal portion of a large-scale, Upper Jurassic fluvial-aeolian system in Paraná Basin, southwestern Gondwana. J. S. Am. Earth Sci. 95, 102248 https://doi.org/10.1016/j. jsames.2019.102248.
- Retallack, G.J., 1988. Field recognition of paleosols. Geol. Soc. Am. Spec. Pap. 216, 1-20.

- Retallack, G.J., 1999a. Postapocalyptic greenhouse paleoclimate revealed by earliest Triassic paleosols in the Sydney Basin, Australia. Geol. Soc. Am. Bull. 111, 52–70.
- Retallack, G.J., 1999b. Permafrost palaeoclimate of Permian palaeosols in the Gerringong volcanic facies of New South Wales. Aust. J. Earth Sci. 46, 11–22.
- Retallack, G.J., 2005. Earliest Triassic claystone breccias and soil-erosion crisis. J. Sediment. Res. 75, 679–695.
- Retallack, G.J., 2021. Multiple Permian-Triassic life crises on land and at sea. Glob. Planet. Chang. 198, 103415.
- Retallack, G.J., Krull, E.S., 1999. Landscape ecological shift at the Permian–Triassic boundary in Antarctica. Aust. J. Earth Sci. 46, 785–812.
- Retallack, G.J., Veevers, J.J., Morante, R., 1996. Global coal gap between Permian–Triassic extinction and Middle Triassic recovery of peat-forming plants. Geol. Soc. Am. Bull. 108, 195–207.
- Retallack, G.J., Smith, R.M.H., Ward, P.D., 2003. Vertebrate extinction across
 Permian–Triassic boundary in Karoo Basin, South Africa. Geol. Soc. Am. Bull. 115,
 1133–1152.
- Retallack, G.J., Metzger, C.A., Greaver, T., Jahren, A.H., Smith, R.M.H., Sheldon, N.D., 2006. Middle-Late Permian mass extinction on land. GSA Bull. 118, 1398–1411.
- Retallack, G.J., Sheldon, N.D., Carr, P.F., Fanning, M., Thompson, C.A., Williams, M.I., Jones, B.G., Hutton, A., 2011. Multiple early Triassic greenhouse crises impeded recovery from late Permian mass extinction. Palaeogeogr. Palaeoclimatol. Palaeoecol. 308, 233–251.
- Rohn, R., Rösler, O., 2000. Middle to Upper Permian phytostratigraphy of the Eastern Paraná Basin. Rev. Un. Guar. 5, 69–73.
- Romer, A.S., Jensen, J.A., 1966. The Chañares (Argentina). Triassic reptiles fauna II. In: Sketch of the Geology of the Río Chañares-Río Gualo region, p. 252. Cambridge.
- Rubidge, B., Erwin, D.H., Ramezani, J., Bowring, S.A., de Klerk, W.J., 2013. High-precision temporal calibration of late Permian vertebrate biostratigraphy: U-Pb zircon constraints from the Karoo Supergroup, South Africa. Geology 41, 363–366.
- Ryberg, P.E., Taylor, E.L., 2012. 439 how productive were the polar forests of the Permian and Triassic of Antarctica? Japan. J. Palynol. 58, 199.
- Ryberg, P.E., Taylor, E.L., Taylor, T.N., 2012. Antarctic glossopterid diversity on a local scale: the presence of multiple megasporophyll genera, Upper Permian, Mt. Achernar, Transantarctic Mountains, Antarctica. Am. J. Bot. 99, 1531–1540.
- Schwendemann, A.B., Decombeix, A.-L., Taylor, E.L., Taylor, T.N., 2010. Collinsonites schopfii gen. et sp. Nov., a herbaceous lycopsid from the Upper Permian of Antarctica. Rev. Palaeobot. Palynol. 158, 291–297.
- Sheldon, N.D., 2005. Do red beds indicate paleoclimatic conditions?: a Permian case study. Palaeogeogr. Palaeoclimatol. Palaeoecol. 228, 305–319.
- Sheldon, N.D., 2006. Abrupt chemical weathering increase across the Permian-Triassic boundary. Palaeogeogr. Palaeoclimatol. Palaeoecol. 231, 315–321.
- Sheldon, N.D., Tabor, N.J., 2009. Quantitative paleoenvironmental and paleoclimatic reconstruction using paleosols. Earth-Sci. Rev. 95, 1–52.
- Sheldon, N.D., Retallack, G.J., Tanaka, S., 2002. Geochemical climofunctions from North American soils and application to paleosols across the Eocene-Oligocene boundary in Oregon. J. Geol. 100, 687–696.
- Sheldon, N.D., Chakrabarti, R., Retallack, G.J., Smith, R.M.H., 2014. Contrasting geochemical signatures on land from the Middle to late Permian extinction events. Sedimentology 61, 1812–1829.
- Shen, Y., Farquhar, J., Zhang, H., Masterson, A., Zhang, T., Wing, B.A., 2011. Multiple S-isotopic evidence for episodic shoaling of anoxic water during late Permian mass extinction. Nat. Commun. 2, 1–5.
- Sidor, C.A., Smith, R.M.H., Huttenlocker, A.K., Peecook, B.R., 2014. New middle Triassic tetrapods from the upper Fremouw Formation of Antarctica and their depositional setting. J. Vertebr. Paleontol. 34 (4), 793–801. https://doi.org/10.1080/ 02724634.2014.837472.
- Simões, M.G., David, J.M., Anelli, L.E., Klein, C., Matos, S.A., Guerrini, V.B., Warren, L. V., 2017. The Permian Tiaraju bivalve assemblage, Passa Dois Group, southern Brazil: biostratigraphic and paleobiogeographic significance. Brazil. J. Geol. 47, 209–224
- Simonson, R.W., 1941. Studies of buried soils formed from till in Iowa. Soil Sci. Soc. Am. Proc. 6, 373–381.
- Smith, R.M.H., 1990. Alluvial paleosols and pedofacies sequences in the Permian lower Beaufort of the southwestern Karoo Basin, South Africa. J. Sediment. Res. 60, 258–276
- Smith, R.M.H., 1995. Changing fluvial environments across the Permian–Triassic boundary in the Karoo Basin, South Africa, and possible causes of the extinctions. Palaeogeogr. Palaeoclimatol. Palaeoecol. 117, 81–104.
- Smith, R.M.H., Botha, J., 2005. The recovery of terrestrial vertebrate diversity in the South African Karoo Basin after the end-Permian extinction. Comp. Rendus Palévol 4, 555–568.
- Smith, R.M.H., Botha-Brink, J., 2014. Anatomy of a mass extinction: sedimentological and taphonomic evidence for drought-induced die-offs at the Permo-Triassic boundary in the main Karoo Basin, South Africa. Palaeogeogr. Palaeoclimatol. Palaeoecol. 396, 99–118.
- Smith, R.M.H., Ward, P.D., 2001. Pattern of vertebrate extinctions across an event bed at the Permian-Triassic boundary in the Karoo Basin of South Africa. Geology 29, 1147–1150. https://doi.org/10.1130/0091-7613(2001)029<1147:POVEAA>2.0. CO:2
- Smith, H., Wilding, L.P., 1972. Genesis of argillic horizons in Ochraqualfs derived from fine textured till deposits of northern Ohio and southern Michigan. Soil Sci. Soc. Am. Proc. 36, 808–815.
- Soares, A.P., Soares, P.C., Holz, M., 2008. Correlações estratigráficas conflitantes no limite Permo-Triássico no sul da Bacia do Paraná: o contato entre duas seqüências e implicações na configuração especial do Aqüífero Guarani. Pesquisas Geoci. 35, 115-133.

- Spalletti, L.A., 1999. Cuencas triásicas del Oeste argentine: origen y evolución. Acta Geol. Hisp. 32. 29–50.
- Spalletti, L.A., Limarino, C.O., 2017. The Choiyoi magmatism in south western Gondwana: implications for the end-permian mass extinction a review. Andean Geol. 44, 328–338.
- Sues, H.-D., Fraser, N.C., 2010. Triassic Life on Land: The Great Transition. Columbia University Press, New York, p. 224.
- Tabor, N.J., Montanez, I.P., 2004. Morphology and distribution of fossil soils in the Permo-Pennsylvanian Wichita and Bowie groups, north-Central Texas, USA: implications for western equatorial Pangean palaeoclimate during icehouse–greenhouse transition. Sedimentology 51, 851–884.
- Tabor, N.J., Montañez, I.P., Steiner, M.B., Schwindt, D., 2007. δ¹³C values of carbonate nodules across the Permian–Triassic boundary in the Karoo Supergroup (South Africa) reflect a stinking sulfurous swamp, not atmospheric CO₂. Palaeogeogr. Palaeoclimatol. Palaeoecol. 252, 370–381.
- Tabor, N.J., Meyers, T.S., Michel, L.A., 2017. Sedimentologist's guide for recognition, description and classification of paleosols. In: Ziegler, K.E., Parker, W.G. (Eds.), Terrestrial Depositional Systems: Deciphering Complexities through Multiple Stratigraphic Methods. Elsevier, Amsterdam, The Netherlands, pp. 165–207.
- Taylor, E.L., Ryberg, P.E., 2007. Tree growth at polar latitudes based on fossil tree ring analysis. Palaeogeogr. Palaeoclimatol. Palaeoecol. 255, 246–264.
- Tewari, R., Chatterjee, S., Agnihotri, D., Pandita, S.K., 2015. Glossopteris flora in the Permian Weller Formation of Allan Hills, South Victoria Land, Antarctica: implications for Paleogeography, Paleoclimatology, and Biostratigraphic Correlation. Gondwana Res. 28, 905–932.
- Torsvik, T.H., Van der Voo, R., Preeden, U., Mac Niocaill, C., Steinberger, B., Doubrovine, P.V., Van Hinsbergen, D.J., Domeier, M., Gaina, C., Tohver, E., Meert, J. G., 2012. Phanerozoic polar wander, palaeogeography and dynamics. Earth Sci. Rev. 114, 325–368.
- Twitchett, R.J., Krystyn, L., Baud, A., Wheeley, J.R., Richoz, S., 2004. Rapid marine recovery after the end-Permian mass-extinction event in the absence of marine anoxia. Geology 32, 805–808.
- Valentine, K.W.G., Dalrymple, J.B., 1975. The identification, lateral variation, and chronology of two buried paleocatenas at Woodhall Spa and West Runton, England. Quat. Res. 5, 561–590.
- Van der Meij, W.M., Temme, A.J.A.M., Lin, H.S., Gerke, H.H., Sommer, M., 2018. On the role of hydrologic processes in soil and landscape evolution modeling: concepts, complications and partial solutions. Earth Sci. Rev. 185, 1088–1106.
- Van Dijk, D.E., 1998. Insect faunas of South Africa from the Upper Permian and the Permian/Triassic Boundary. Palaeontol. Afr. 34, 34–38.
- Van Dijk, D.E., Geertsema, H., 1999. Permian insects from the Beaufort Group of Natal, South Africa. Ann. Natal Mus. 40, 137–171.
- Van Hinsbergen, D.J.J., de Groot, L.V., van Schaik, S.J., Spakman, W., Bijl, P.K., Sluijs, A., Langereis, C.G., Brinkhuis, H., 2015. A paleolatitude calculator for paleoclimate studies. PLoS One 10, e0126946. https://doi.org/10.1371/journal. pone.0126946.

- Veevers, J.J., Saeed, A., 2007. Central Antarctic provenance of Permian sandstones in Dronning Maud Land and the Karoo Basin: Integration of U–Pb and T_{DM} ages and host-rock affinity from detrital zircons. Sediment. Geol. 202, 653–676.
- Viglietti, P.A., 2020. Biostratigraphy of the Daptocephalus Assemblage Zone (Beaufort Group, Karoo Supergroup), South Africa. South African J. Geol. 123 (2), 191–206.
- Viglietti, P.A., Rubidge, B.S., Smith, R.M.H., 2017. Revised lithostratigraphy of the Upper Permian Balfour and Teekloof formations of the main Karoo Basin, South Africa. S. Afr. J. Geol. 120, 45–60. https://doi.org/10.25131/gssajg.120.1.45.
- Viglietti, P.A., Smith, R.M.H., Rubidge, B.S., 2018. Changing palaeoenvironments and tetrapod populations in the *Daptocephalus* Assemblage Zone (Karoo Basin, South Africa) indicate early onset of the Permo-Triassic mass extinction. J. Afr. Earth Sci. 138, 102-111
- Wachbuscha, P., Korsch, R.J., Beaumonta, C., 2009. Geodynamic modelling of aspects of the Bowen, Gunnedah, Surat and Eromanga Basins from the perspective of convergent margin processes. Aust. J. Earth Sci. 56, 309–334.
- Ward, P.D., Montgomery, D.R., Smith, R.M.H., 2000. Altered river morphology in South Africa related to the Permian-Triassic extinction. Science 289, 1740–1743. https://doi.org/10.1126/science.289.5485.1740.
- Ward, P.D., Botha, J., Buick, R., DeKock, M.O., Erwin, D.H., Garrison, G., Kirschvink, J., Smith, R.M.H., 2005. Abrupt and gradual extinction among late Permian land vertebrates in the Karoo Basin, South Africa. Science 307, 709–714. https://doi.org/ 10.1126/science.1107068.
- Weissmann, G.S., Hartley, A.J., Nichols, G.J., Scuderi, L.A., Olson, M.E., Buehler, H.A., Banteah, R., 2010. Fluvial form in modern continental sedimentary basins: distributive fluvial systems. Geology, b. 38, 39–42.
- Weissmann, G.S., Hartley, A.J., Scuderi, L.A., Nichols, G.J., Davidson, S.K., Owen, A., Atchley, S.C., Bhattacharyya, P., Chakraborty, T., Ghosh, P., Nordt, L.C., Michel, L., Tabor, N.J., 2013. Prograding distributive fluvial systems-geomorphic models and ancient examples. In: Driese, S.G., Nordt, L.C., McCarthy, P.J. (Eds.), New Frontiers in Paleopedology and Terrestrial Paleoclimatology-Paleosols and Soil Surface Analog Systems. SEPM Special Publication No. 104, pp. 131–147.
- Whitney, M.R., Sidor, C.A., 2020. Evidence of torpor in the tusks of Lystrosaurus from the early Triassic of Antarctica. Commun. Biol. 3, 471 doi.10.1038/s42003-020-01207-6
- Xu, H., Veblen, D.R., 1996. Interstratification and other reaction microstructures in the chlorite-berthierine series. Contrib. Mineral. Petrol. 124, 291–301.
- Yu, J., Broutin, J., Chen, Z.Q., Shi, X., Li, H., Chu, D., Huang, Q., 2015. Vegetation changeover across the Permian-Triassic Boundary in Southwest China: extinction, survival, recovery and palaeoclimate: a critical review. Earth Sci. Rev. 149, 203–224.
- Zerfass, H., Chemale Jr., F., Schultz, C.L., Lavina, E., 2004. Tectonics and sedimentation in Southern South America during the Triassic. Sediment. Geol. 166, 265–292.
- Zhang, G., Buatois, L.A., Mángano, M.G., Aceñolaza, F.G., 1998. Sedimentary facies and environmental ichnology of a ?Permian playa-lake complex in western Argentina. Palaeogeogr. Palaeoclimatol. Palaeoecol. 138, 221–243.